FUNCTIONAL NITROXYLS IN POLYPROPYLENE BASED THERMOPLASTIC VULCANIZATES

by

Michael Walker Bodley

A thesis submitted to the Department of Chemical Engineering

In conformity with the requirements for

the degree of Master of Applied Science

Queen's University

Kingston, Ontario, Canada

(May, 2017)

Abstract

Peroxide vulcanization of polypropylene (PP) based thermoplastic vulcanizates (TPVs) is hindered by PP's susceptibility to radical degradation. PP degradation occurs through chain scission of tertiary alkyl macroradicals, reducing molecular weight, and negatively effecting TPV blend morphology. Nitroxyl chemistry using acryloyloxy-2,2,6,6-tetramethylpiperidine-N-oxyl (AOTEMPO) was exploited to control the dynamics and rheological outcomes of peroxide polyolefin modifications. PP melt viscosity was partially retained by introducing a competition between macromonomer oligomerization and β-scission. Further improvements were observed when synergizing the polymer-bound acrylate functionality of AOTEMPO, with trimethylolpropane triacrylate (TMPTA) a multifunctional coagent. Resulting TPVs contained smaller, more dispersed crosslinked elastomer particles when compared to peroxide-only formulations, owing to the retention of PP molecular weight.

A follow up investigation into the effects of AOTEMPO on TPV physical property performance was completed for low elastomer content blends (0-20wt%). AOTEMPO formulations provided improved particle dispersion compared to peroxide only formulations, owing to the retention of melt viscosity. These improved particle dispersions led to better impact performance for AOTEMPO formulations over peroxide only formulations. Additionally, AOTEMPO formulations provided improved tensile properties compared to peroxide only formulations, owing to the branched architecture formed during polyolefin modification.

Acknowledgements

I would like to thank my supervisor, Dr. Scott Parent, for providing me with an opportunity to study a new field, and enabling me to develop my critical thinking skills. His support and guidance was instrumental in completing this degree. I would like to thank my lab mates: Kyle, Kelli, Karolina, Rachel, Stu, Praphulla, Othmane, and the rest of the Parent research group for making my time in the lab all the more enjoyable. I wish all of you the best of luck moving forward.

I would like to thank Dr. Marianna Kontopoulou for allowing me to use her polymer processing equipment, and providing me the opportunity to assist in developing and delivering the 3rd design course content. I would also like to thank Professor Dave Mody for providing advice throughout my journey to become a professional engineer.

Final and most importantly, I would like to thank my family. Without them I would not be where I am today.

Table of Contents

List of Figures

List of Tables

List of Abbreviations

AOTEMPO – 4-acryloyloxy-2,2,6,6-tetramethylpiperidine-N-oxyl

DCP – dicumyl peroxide

DV – dynamic vulcanization

EOC – poly(ethylene-co-octene)

EPDM – ethylene propylene diene

G' – storage modulus

G" – loss modulus

hr – hours

Hz – hertz

Irganox 1010 – pentaerythritol tetrakis(3,5-di-tert-butyl-4-hydroxyhydrocinnamate)

L130 - 2,5-bis(tert-butylperoxy)-2,5-dimethyl 3-hexyene

LCB – long chain branching

lit- literature

LLDPE – linear low density polyethylene

MFR – melt flow rate

min – minutes

mp – melting point

η* – complex viscosity

PDI – polydispersity index

PP – polypropylene

RPM – rotations per minute

SEM – scanning electron microscopy

TEMPOH - 4-hydroxy-2,2,6,6-tetramethylpiperidin-1-oxyl

TMPTA – trimethylolpropane triacrylate

TPEs – thermoplastic elastomers

TPOs – thermoplastic olefins

TPVs – thermoplastic vulcanizates

TR – trapping ratio

μm – micrometers

μmol – micromoles

List of Schemes

Chapter 1

Introduction

1.1 Thermoplastic Vulcanizates

Mixing a thermoplastic with an elastomer to produce a thermoplastic olefin blend (TPO) has become a common industrial process. A leading example is rubber toughening, wherein a brittle material such as polypropylene (PP) is compounded with an elastomeric polyolefin such as ethylene propylene diene monomer (EPDM) or, more recently, with ultra-low-density metallocene ethylene-α-olefin copolymers [1], [2]. Chemical modification of these blends during melt compounding, a process called dynamic vulcanization (DV), can yield a crosslinked elastomer phase that is dispersed within the thermoplastic matrix[3], [4]. These reacted polymer blends are known as thermoplastic vulcanizates (TPVs), and are valued commercially for their enhanced mechanical properties, chemical resistance, melt strength, and thermal stability. They can be processed in the melt state using standard polymer compounding equipment without concern for changes of dispersed phase morphology.

1.2 Blend Morphology

DV is a complex process wherein blend morphology is established concurrently with polyolefin modification. End-use properties are sensitive to the size and distribution of the elastomer phase, with highly dispersed particles of sub-micron diameter being favoured. Research into unreactive polymer blends[5]–[7] has identified two key variables that affect morphology development: the viscosity (μ) of the parent materials, and the relative abundance of the components (typically evaluated by the volume fraction, φ). Additional factors include the interfacial tension between

components, the nature and amount of additives (stabilizers, accelerators, etc), and the processing conditions generated by the mixing device (shear rate, temperature, equipment geometry)[3].

The morphology of an immiscible blend can be visualized as an unstabilized emulsion, whose coalescence into large macro-phases is hindered by the high viscosity of its components (Figure 1(a)). As the content of the dispersed phase material is increased, the average droplet size is observed to increase, until a critical value is reached that causes a shift toward a co-continuous morphology (Figure 1(b)).

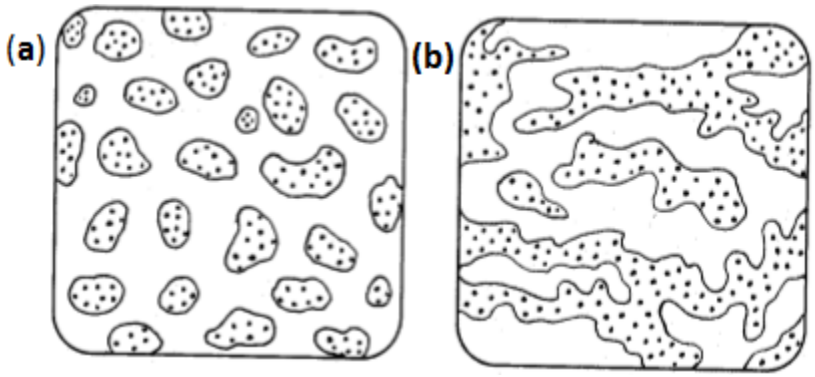

Figure 1 – Visualization of a dispersed blend morphology (a), and a co-continuous blend morphology (b)[3]

During melt mixing of inert blends, two competing mechanisms occur, droplet breakup and droplet coalescence, with material loadings, viscosities, and processing conditions dictating the final morphology. In the case of DV, polyolefin modification affects the melt viscosity of the starting materials, thereby shifting the steady-state morphology of the blend. Crosslinking of the elastomer phase raises its viscosity, while changes in thermoplastic phase depend on the cure formulation employed. In cases of low rubber content TPVs (<20wt%), the thermoplastic will

comprise the continuous phase throughout DV, since the volume fraction is dominant. In cases of high rubber content TPVs (60-80%), the elastomer starts out as the continuous phase, but an increase its viscosity leads to phase inversion. The final product has the thermoplastic as continuous matrix, despite being the minor component[8]. Providing a significant crosslink density is achieved, the elastomer is rendered thermoset, preventing its coalescence into larger dispersed phase domains. Thus the blend morphology is “locked”; a major advantage over unreacted blends[3].

1.3 Vulcanization Chemistry

PP/EPDM TPVs are a mature commercial technology, having been studied for nearly 50 years. A variety of crosslinking agents have been employed to manufacture these materials including: sulfur vulcanization, peroxide-initiated vinyltrialkoxysilane (VTES) grafting + moisture-curing, phenol-formaldehyde resins, and peroxide-initiated curing. Each crosslinking system has its advantages and disadvantages.

Sulfur cures can provide exceptional dynamic mechanical properties, owing to the labile polysulfide bonds that comprise the covalent network. Furthermore, sulfur curing can only operate on polymers containing unsaturation, allowing for selective curing of EPDM, while leaving PP unmodified. However, due to curing requirements, and the small amount of unsaturation present in EPDM, sulfur cures often require inorganic and organic additives to accelerate the vulcanization rate and boost crosslinking yields[9].

Fritz et al. [10] produced a PP-based TPV using moisture-curing chemistry to generate the requisite crosslink density. A poly(ethylene-co-octene) (EOC) material was graft-modified by

radical addition of vinyltriethoxysilane (VTES) before being melt-compounded with PP. The EOC-g-VTES phase was crosslinked by hydrolysis/condensation chemistry under intense mixing. The TPV product displayed no discolouration, and possessed excellent viscoelastic and tensile properties. Despite this apparent success, additional literature on this technology is limited to a few patents[11].

Activated phenol-formaldehyde resins, commonly referred to as resol resins, are amongst the most common crosslinking agents used in TPV manufacturing. This EPDM cure chemistry was studied extensively by Van Duin et al[9], [12], [13], using 2-ethylidene norbornane as a low molecular weight model compound. A common resol resin formulation contains a reactive alkylphenolic resin that acts as the crosslinking agent, a halogen containing compound, and a Lewis acid catalyst such as zinc chloride or ferric chloride. Electrophilic addition of cationic intermediates to the C=C unsaturation within EPDM generates crosslinks[12], [13]. Two major disadvantages with this cure system are the tendency to absorb moisture, thus requiring high temperature drying procedures before processing, and dark brown discolouration of the cured product[3].

Peroxide formulations can crosslink saturated and unsaturated elastomers at predictable rates without concern for cure reversion [3,10]. This is essential for the TPVs derived from elastomers such EOC, which have attracted interest due to their narrow molecular weight distributions, uniform co-monomer distributions and short-chain branched architectures [2], [14]. These materials lack the unsaturation needed to support sulfur or resin cures, necessitating the use of some form of radical chemistry. The challenge in applying peroxides to PP-based TPV

formulations is the susceptibility of the thermoplastic to radical degradation. This undesirable side reaction of PP can result in severe losses in matrix molecular weight, which can compromise material properties.

1.4 Peroxide-Initiated Polyethylene Curing Fundamentals

Scheme 1 shows the mechanism of peroxide-initiated crosslinking of ethylene-rich polymers. Irreversible thermolysis of dicumyl peroxide (DCP) at high temperature produces cumyloxy radicals whose fate depends on the availability of H-atom donors. Polymers containing labile C-H bonds engage cumyloxyl in H-atom transfer to give cumyl alcohol and a macroradical, whose termination by combination produces the desired C-C crosslink. Macroradical generation competes with cumyloxy radical fragmentation to give acetophenone and a methyl radical[15], the latter being much less reactive than alkoxyl radicals toward H-atom abstraction.

Since radicals are generated in pairs and terminate in pairs, this simple crosslinking can yield a maximum of one crosslink per molecule of peroxide. However, given limitations on the macroradical yield and the propensity of alkyl macroradicals to terminate by disproportionation, the crosslink yield is a fraction of the maximum stoichiometric yield. The exact crosslink yield is a function of polymer structure, due to differences in H-atom donor reactivity, and macroradical termination preferences.

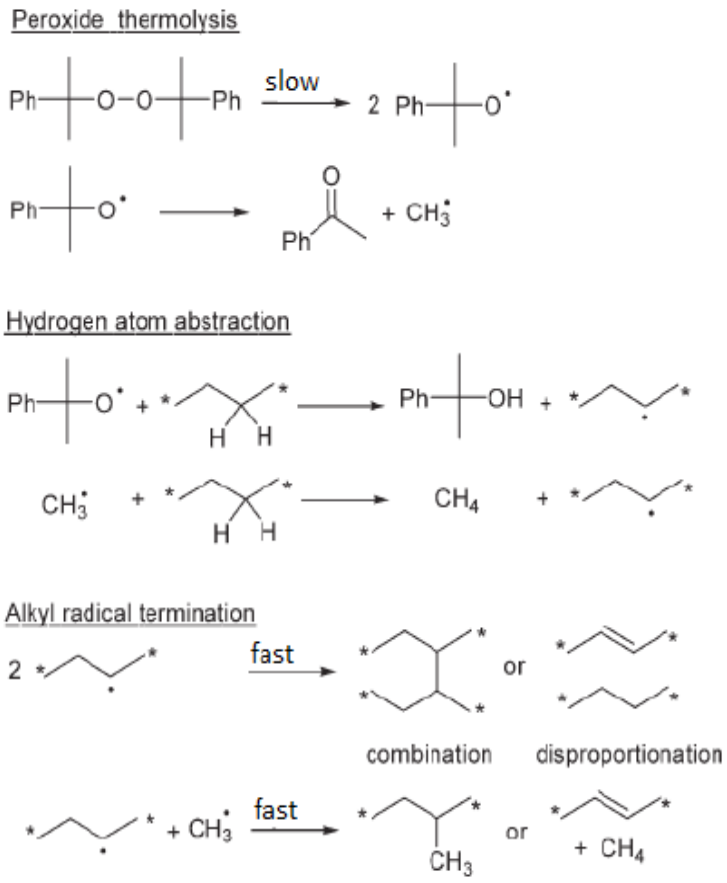

Scheme 1 - Stoichometric crosslinking of ethylene-rich materials[16]

The overall dynamics of peroxide cures are dictated by initiator thermolysis, since radical-radical termination has a very low activation energy, and proceeds at the diffusion limit of reaction velocities [17], [18]. Given that peroxide decomposition follows first order kinetics, the highest reaction rate occurs in the initial stages of the cure, and it declines with initiator conversion. These cure dynamics can be observed by monitoring changes in the storage modulus (G') at constant temperature, frequency and strain amplitude[19], as illustrated in Figure 2 for a DCP-

initiated cure of linear low density polyethylene (LLDPE). This rheological method of quantifying cure dynamics is based on the sensitivity of G' to crosslinking density, which restricts polymer chain segment mobility and enhances melt elasticity [20]. Changes in G' are generally observed to be proportional to initiator conversion, confirming that initiator decomposition is the rate determining step of the process.

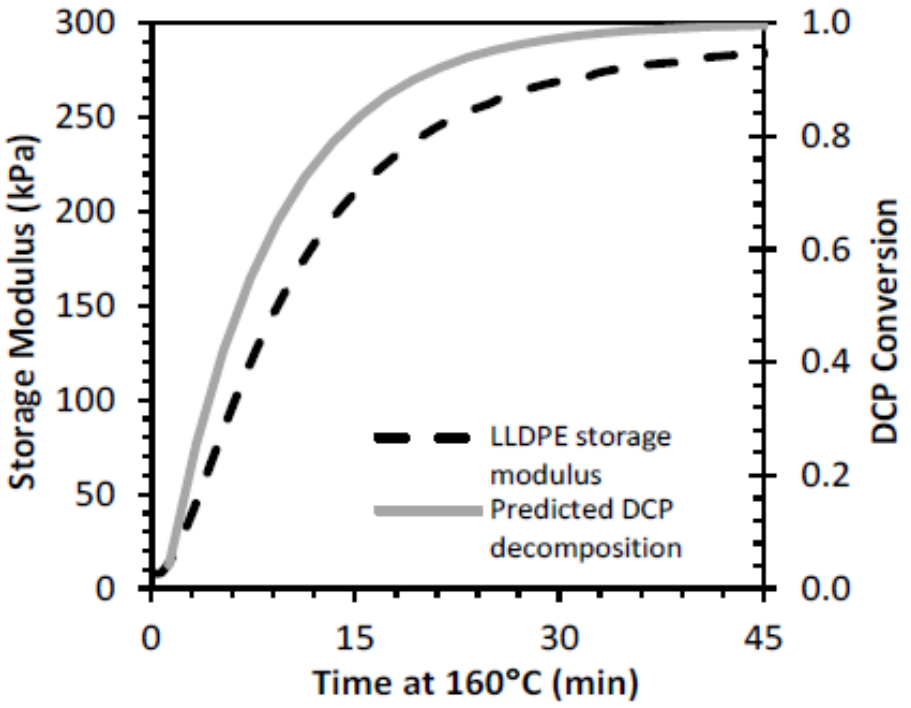

Figure 2 – Comparison between change in G' and conversion of initiator for LLDPE curing[21]**.**

1.5 Polypropylene Degradation

It is well established that PP degrades in the presence of peroxides (Scheme 2)[22], [23], resulting in a substantial loss of molecular weight and melt viscosity. H-atom abstraction occurs predominantly from tertiary C-H bonds, as opposed to secondary and primary sites contained

within a PP homopolymer [24]. Degradation is attributed to β-scission of tertiary alkyl macroradcials, which occurs without loss of radical concentration. As a result, PP cleavage has a kinetic chain character that outcompetes crosslinking by combination reactions of primary and secondary alkyl radicals [25]. Moreover, this scission process has a significant activation energy, making it more problematic at elevated temperatures needed to melt and process polypropylene for TPV manufacturing [26].

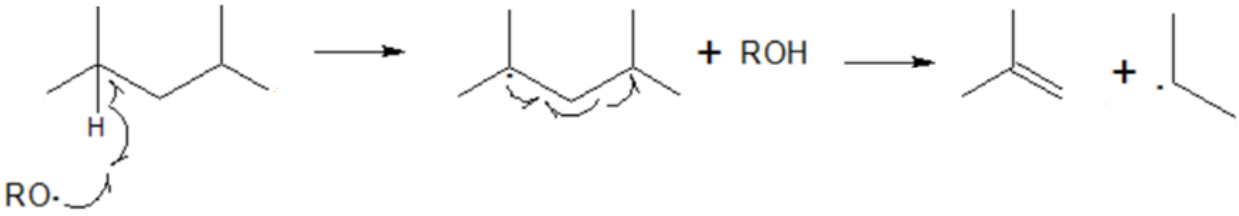

Scheme 2 – Peroxide initiated degradation of polypropylene

PP degradation can be detrimental to TPV production, as reductions in melt viscosity often lead to coarser blend morphologies that result in poorer physical properties. Researchers have investigated the use of multifunctional reactive compounds, commonly known as coagents, in an attempt to mitigate the effects of β-scission.

1.6 Coagent-Mediated Vulcanization

Coagents are widely used to accelerate and improve the yield of peroxide-initiated elastomer curing [27]. They can be classified into two groups. Type I coagents include acrylates, styrenics, and maleimide-based additives that react rapidly at common cure temperatures. Radical oligomerization of the C=C functionality within these coagents occurs through a closed propagation sequence that does not consume radical intermediates[28], allowing for complete reagent consumption at the expense of minimal initiator radicals. Examples of Type I coagents include trimethylolpropane triacrylate (TMPTA), divinyl benzene (DVB) and N,N'-m-phenyl

dimaleimide. Type II coagents raise crosslink densities without affecting the initial cure rates substantially. Examples include triallyl cyanurate (TAC), triallyl phosphate (TAP) and triallyl trimesate (TAM)[29].

Although coagents are traditionally used to boost crosslink density of thermosets, attempts have been made to apply them to PP:EOC TPVs[30], [31] to minimize radical degradation. While they report improved particle dispersions and mechanical properties achieved with the employment of a coagent[30]–[32], further research into the effects of coagents on PP homopolymer modification is needed to gain insight into TPV manufacturing.

A series of works was published on introducing long chain branching (LCB) to PP using peroxides and allylic coagents at elevated temperatures[33]–[37]. Their aim was to transform linear chains into branched materials by off-setting the effects of β-scission with coagent-induced crosslinking. However, it was observed that the bulk molecular weight distribution shifted and narrowed with degradation, and a small bimodal distribution of highly branched PP was formed[34]. These results suggest that radical activity is concentrated on the larger chains of the molecular weight distribution[38], and cleavage of linear PP chains into smaller fragments makes it challenging to introduce uniform branching (Scheme 3).

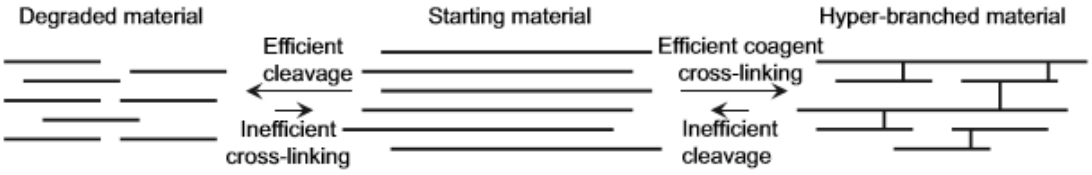

Scheme 3 – Coagent induced bimodality of PP chains[34]

It the context of TPVs, the inefficient grafting capabilities of coagents will result in large scale degradation of the PP matrix with little melt viscosity retention. Reductions in PP molecular weight often lead to coarser morphologies compared to their unreacted counterpart, and poorer tensile properties, since there are less chain entanglements [39], [40]. These facts have motivated us to find new strategies for preserving PP molecular weight, and melt viscosity, in an attempt to produce superior TPVs with finer particles sizes and dispersion, and retained tensile properties.

1.7 AOTEMPO-Mediated Curing of Polyethylene

Functionalized nitroxyls, such as acryloyloxy-2,2,6,6-tetramethylpiperidine-N-oxyl (AOTEMPO) have been developed to control the dynamics and yields of LLDPE cures [41], [42]. Figure 3 provides a comparison between a stoichiometric cure, and an AOTEMPO-mediated cure formulation. When a nitroxyl is added to a cure formulation, alkyl macroradicals generated by H-atom abstraction are quenched by nitroxyl, providing an induction period (phase 1). Post induction, lost crosslink density is recovered by functional group activation of polymer bound acrylate functionality, forming macromonomer oligomers through a kinetic chain reaction (phase 2). Upon complete conversion, stoichiometric curing continues until the remaining initiator is consumed. These reactions have been shown to be compatibility with coagents, providing typical boosts in crosslink density without affecting cure dynamics[42].

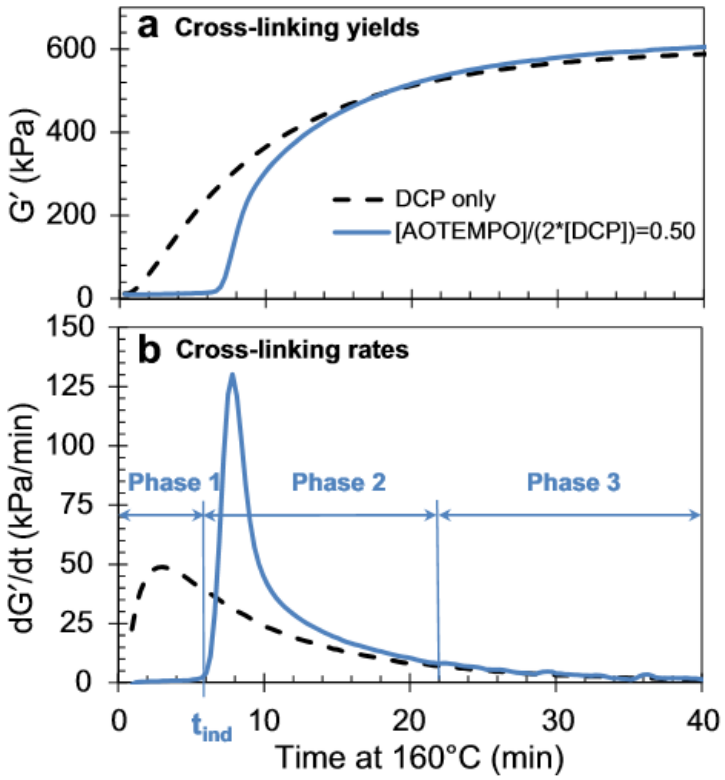

Figure 3 – Difference in dynamics between initiator only, and AOTEMPO-mediated crosslinking of LLDPE[42]

Scheme 4 illustrates the essential elements of an AOTEMPO-mediated polyethylene cure. Since it requires H-atom transfer from the polymer to peroxide-derived alkoxy radicals, an initiator's abstraction efficiency is a key process variable. Fragmentation of cumyloxyl leads ultimately to methyl alkoxyamines that can be rendered polymer-bound during the acrylate oligomerization phase of the process, but do not otherwise contribute to crosslink density. Note that the oligomerization of acrylate groups during phase 2 can be accompanied by alkyl macroradical combination, with both processes contributing to crosslink density. Once all acrylate functionality is consumed, secondary alkyl macroradical combination continues to build network density.

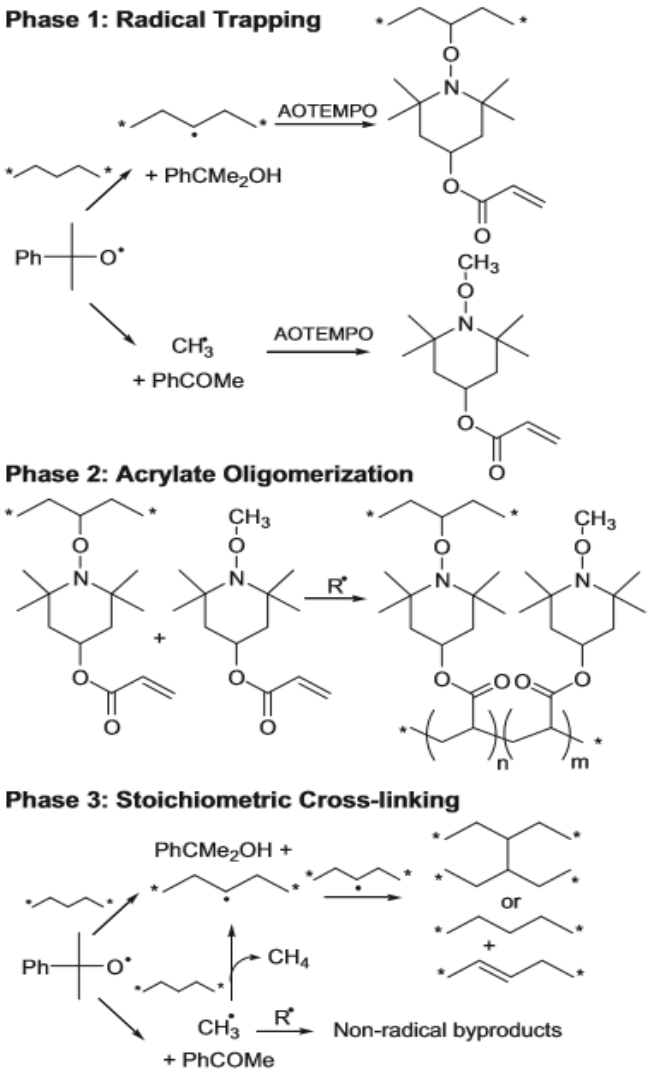

Scheme 4 – Principle reactions underlying AOTEMPO-mediated PE curing[42]

AOTEMPO chemistry has eliminated many limitations of conventional polyethylene crosslinking processes, and a simple extension of this approach may overcome broader issues associated with peroxide cure technology. Adapting this chemistry for PP modifications has shown considerable promise in terms of mitigating chain scission effects[16]. In this case, phase 1 yields macromonomer functionality that is oligomerized in phase 2 to build a crosslink network. This

oligomerization process competes with chain scission, the balance of which dictates the ultimate crosslink density. Phase 3 is to be avoided for PP systems, in that uncontrolled polymer modification serves only to degrade the material, unlike the polyethylene system whose natural tendency is to crosslink. This strategy has the potential to affect control over PP reaction outcomes such that molecular weight losses are not an inevitable outcome of a peroxide-initiated process, but can be controlled to the extent that is required by the final application.

1.8 Research Objectives

The focus of this research will be to evaluate the merits of AOTEMPO technology for the preparation of PP-based TPVs. Specific goals include:

1. Manufacturing of TPVs with a continuous PP matrix that demonstrate melt-state rheological properties that approach those of the starting material.
2. Control the dynamics of PP:EOC dynamic vulcanization to produce finer EOC particle dispersions.
3. Assess the impact resistance and mechanical stiffness of PP:EOC TPVs against appropriate controls.

Chapter 2

AOTEMPO-Mediated Manufacturing of TPVs

2.1 Introduction

TPV manufacturing is a reactive blending process in which phase morphology evolves concurrently with chemical modification of one or both polymer components. Our objective was to explore the potential of functional nitroxyls to facilitate TPV production by radical chemistry, with success defined as a continuous PP phase whose rheological properties approach those of the starting material, and a finely-dispersed crosslinked EOC phase. These studies begin with an examination of individual polyolefin reactivity to establish the sensitivity of polymer modification dynamics and yields to potential formulation components. This is followed by studies of the dynamic vulcanization of PP:EOC blends, with particular emphasis on TPV morphology and melt-state rheological properties.

2.2 Experimental

2.2.1 Materials

A commercial grade poly(ethylene-co-octene) (Engage 8003), containing 7.6 mol% octane[43], with a density of 0.885 g/cm^3, and a MFR of 1.0 g/10min at 190°C was supplied by DOW Chemical. Polypropylene, Pro-fax 6523, with a weight average molecular weight of 340 kg/mol[44], a density of 0.9 g/cm^3, and a MFR of 4.0 g/10 min at 230°C was used as received from LyondellBasell, USA. Dicumyl peroxide (DCP, 99%), acryloyl chloride (≥97%), triethylamine (≥99%), 4-hydroxy-2,2,6,6-tetramethylpiperidin-1-oxyl (TEMPOH, 97%), trimethylolpropane triacrylate (TMPTA, 98%), and pentaerythritol tetrakis(3,5-di-tert-butyl-4-hydroxyhydrocinnamate) (Irganox1010, 98%) were used as received from Sigma-Aldrich.

2.2.2 AOTEMPO Synthesis

A solution of triethylamine (706 mg, 0.97 mL, 6.98 mmol) in benzene (12.0 mL) was added dropwise to a solution of TEMPOH (0.688 g, 4.40 mmol) in benzene (10.0 mL). Acryloyl chloride (0.374 g, 340 µL, 4.16 mmol) in benzene (7.0 mL) was added dropwise at room temperature, under N_2 with stir. The reaction was stirred at room temperature for 20 h before the second portion of acryloyl chloride (0.188 g, 170 µL, 2.08 mmol) in benzene (3.5 mL) was added dropwise. The reaction was stirred at room temperature for an additional hour. Resulting solution was filtered before removing solvent under vacuum, yielding orange crystals that were recrystallized from cyclohexane. Yield: 76%; mp 100-102 °C; lit. 102-104 °C[45].

2.2.3 TPV Synthesis

PP:EOC blends (by weight, 80:20, 70:30, 60:40, 50:50) were prepared using a Haake Polylab R600 internal batch mixer. EOC (40 g) was mixed with the required curatives (Table 1) at 90 °C and 60 rotations per minute (RPM) for 5 min to produce EOC+curative masterbatches, which were removed from the device and cut into pellets. The required amount of PP was charged to the mixer at 180 °C, and mixed at 60 RPM for four minutes, before adding the required amount of EOC masterbatch. Mixing continued for an additional 5 min at 60 RPM before the addition of Irganox 1010 (0.5 wt%, 4.25 µmol/g). By specific example, 70:30 TPVs were prepared by mixing DCP (0.333 g, 1232 µmol) TMPTA (1.333 g, 4500 µmol) and AOTEMPO (0.435 g, 1924 µmol) into 40 g of EOC to provide the concentrations outlined in Table 1. Twelve grams of EOC containing DCP (0.1 g, 370 µmol), TMPTA (0.4 g, 1350 µmol), and AOTEMPO (0.1305g, 577 µmol) was then mixed into 28 g of molten PP, providing the desired DCP (9.25 µmol/g), TMPTA (33.75 µmol/g), and AOTEMPO (12 µmol/g) concentrations. Unreactive blends were quenched using ice-water to preserve the morphology and avoid annealing.

Table 1 – EOC masterbatch compositions

Blend Composition (PP:EOC)	80:20	70:30	60:40	50:50
DCP Loading (µmol/g)	46.2	30.8	23.1	18.5
TMPTA Loading (µmol/g)	168.7	112.34	84.25	67.5
AOTEMPO Loading (µmol/g)	60.1	48.1	36.1	24.0

2.2.4 Rheological Analysis

Individual PP or EOC formulations were reacted in the cavity of a controlled-strain rheometer (Advanced Polymer Analyzer 2000, Alpha Technologies) equipped with biconical plates operating at 180 °C, 1 Hz, 3° arc. Samples were prepared by grinding the polymer (5 g), and coating the resulting powder with an acetone solution of the desired reagents. The resulting mixtures were hand-mixed before allowing the acetone to evaporate, and introducing the material to the rheometer.

The dynamic rheological properties of TPV samples were measured with a controlled strain rheometer (Anton Parr MCR301) equipped with 25 mm parallel plates, using a 1 mm gap at 170 °C, and 3% strain. Stress sweeps were performed to ensure that data acquired was within the linear viscoelastic region.

2.2.5 TPV Morphology Imaging

Samples were immersed in liquid nitrogen for 5 min before fracturing. Surfaces of interest were etched for 2.5 hr using heptane at 80 °C. Unreacted blends were immediately dried under vacuum at 60 °C for 10 hr, while TPVs were sonicated using a Misonix XL2000 microson ultrasonic probe for three 1 min intervals at a power output of 22 watts before drying. All etched samples were gold-coated and imaged using a Hitachi S-2300 scanning electron microscope. Images were

analyzed using ImageJ, imaging analysis software, to estimate the mean diameter of the dispersed elastomer phase, as well as the polydispersity index (PDI). PDI was calculated using the following formulas [46]:

$$PDI = \frac{D_w}{D_n} \qquad D_n = \frac{\sum_{i=1}^{n} n_i D_i}{\sum_{i=1}^{n} n_i} \qquad D_w = \frac{\sum_{i=1}^{n} n_i D_i^4}{\sum_{i=1}^{n} n_i D_i^3}$$

2.3 Results and Discussion

2.3.1 Modification of Individual Blend Components

The outcome of a conventional peroxide modification is dictated by the intrinsic reactivity of alkyl macroradical intermediates. In the case of ethylene-rich polyolefins, macroradical combination is the dominant molecular weight-altering reaction, resulting in polymer crosslinking through C-C bond formation. In the case of propylene-rich polyolefins, β-scission of tertiary macroradicals overwhelms macroradical termination by combination, and peroxide modification of PP homopolymers generally results in large-scale degradation. Therefore, the synthesis of a TPV comprised of crosslinked EOC that is dispersed within a high viscosity PP matrix runs contrary to the inherent reactivity of our polyolefins.

Further challenges arise from the inherent dynamics of peroxide-initiated polyolefin modifications. All of these processes generate radicals through initiator thermolysis, a first-order reaction with a rate constant on the order of 10^{-2} s^{-1} at conventional polymer processing temperatures. Subsequent radical termination by combination and/or disproportionation is diffusion-controlled, with bimolecular rate constants on the order of 10^{8}-10^{9} $M^{-1}s^{-1}$[17], [18]. Since peroxide decomposition is rate determining, overall process dynamics are inherently first-order, with reactions proceeding fastest in the initial stages, when the peroxide concentration is

highest, and slowing exponentially as the initiator decomposes. Since TPV synthesis involves simultaneous polymer modification and blend morphology evolution, intrinsically high initial reaction rates may be problematic.

Consider the rheology data plotted in Figure 4 for the peroxide-initiated modification of EOC and PP. As stated earlier G' measurements, recorded at a fixed temperature, frequency, and shear strain amplitude, are a standard means of monitoring the progress of reactions that affect polymer architecture[19]. An EOC formulation comprised of DCP alone crosslinked with characteristic first-order kinetics (Figure 4a), curing quickly once the polymer reached the reaction temperature. Since the half-life of DCP at 180°C is 0.86 min, the process was essentially complete after 10 min, resulting in a net gain in G' of 150 kPa (gel content 62.3%). In contrast, a DCP-only formulation of PP resulted in substantial polymer degradation, with a net loss in G' of -12 kPa over the same period (Figure 4b).

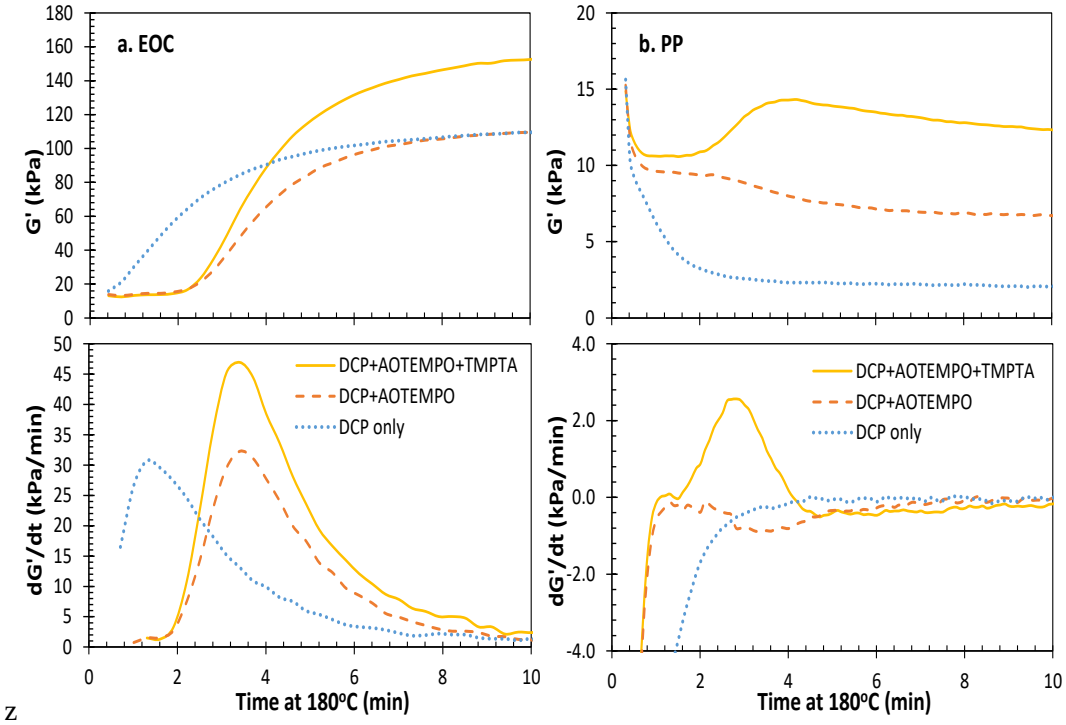

z

Figure 4 - Evolution of G' and dG'/dt for peroxide-initiated polyolefin reactions at 180 ºC, 1Hz, 3° arc (a. EOC; b. PP; [DCP]= 9.25 µmol/g; TR=0.65; [TMPTA]= 33.75 µmol/g)

The ability of functional nitroxyls such as AOTEMPO to provide a measure of control over the dynamics and yields of polyolefin modifications has been demonstrated previously[21], [41], [42]. These reactions progress through a sequence of three phases; induction, C=C oligomerization, and uncontrolled polymer modification. During the induction phase, trapping of carbon-centered radicals by combination with nitroxyl quenches macroradical intermediates. Since the polymer's molecular weight distribution remains constant until all nitroxyl is consumed, the induction time is a simple function of the peroxide half-life and the amount of AOTEMPO charged to the formulation. The latter is generally expressed as the trapping ratio, TR = [AOTEMPO]/(2*[DCP]), which represents the fraction of initiator-derived radicals that will be

quenched by the additive. In general, the induction time is not a function of polyolefin structure, as indicated by a comparison of DCP+AOTEMPO rheology data for EOC and PP in Figure 4a,b.

The second phase of an AOTEMPO process builds a polymer network by oligomerization of polymer-bound acrylate functionality. In the case of EOC, the cure rate is accelerated relative to peroxide alone, since C-C bond formation occurs by functional group activation as well as macroradical combination (Figure 4a). In the case of PP, crosslinking competes with macroradical scission, the balance of which dictates the net change in storage modulus. This balance is affected by polymerizable group structure, trapping ratio, and initial PP molecular weight. Although the DCP+AOTEMPO formulation illustrated in Figure 4b incurred a small extent of degradation, formulations can be designed to meet a range of product architectures, from degraded to slightly branched to thermoset.

Phase three of the process, uncontrolled modification, is marked by the complete conversion of acrylate functionality, at which point residual peroxide further crosslinks EOC (DCP+AOTEMPO gel content 72.1%), and further degrades PP. Optimization of the trapping ratio can minimize this stage by supplying only as much initiator as is required to convert polymer-bound C=C functionality. Given the current state of knowledge, this optimal trapping ratio can only be determined by trial and error experimentation.

A simple means of promoting polyolefin crosslinking exploits the synergy between AOTEMPO and trifunctional coagents such as TMPTA. Copolymerization of polymer-bound acrylate groups and TMPTA during the oligomerization phase yields a more extensive C-C network that raises

the crosslink density of EOC formulations (DCP+AOTEMPO+TMPTA gel content 82.9%), and can shift the outcome of a PP modification from degradation to crosslinking (Figure 4). The challenge in developing a TPV synthesis is to find a peroxide concentration, coagent loading, and nitroxyl trapping ratio that provide the requisite induction time, EOC crosslink density and PP matrix viscosity. The initiator and AOTEMPO concentrations used to generate Figure 4 ([DCP]=9.25 μmol/g, TR=0.65) were selected from a series of preliminary EOC and PP experiments that were designed to generate an induction delay of 1.8 min, and favourable polyolefin modification outcomes. It should be noted, however, that conditions within the rheometer cavity differ from those generated by an internal mixer, and the TPV experiments described below may benefit from further optimization.

2.3.2 TPV Synthesis and Properties

A leading application of TPV technology is impact-modified polypropylene, which is comprised of a thermoplastic PP matrix and well-dispersed thermoset elastomer[47]. The thermomechanical properties of this class of TPVs are sensitive to a wide range of variables, including the molecular weight distribution of the PP matrix, as well as the size and crosslink density of the elastomer phase. Ideally, the PP matrix is unchanged by the cure formulation, while the EOC phase is distributed uniformly as crosslinked particles with submicron dimensions[3].

The synthesis of a TPV is a complex exercise in reactive polymer processing, in which blend morphology is established concurrently with chemical modification of the constituent polyolefins. Decisions regarding material selection, and processing conditions such as mixing protocol, shear stresses imposed during DV, and relative timescale of morphology development and radical chemistry are influential on TPV manufacturing. Naskar et al[48], have shown that the sequence

of polymer and curative addition to the mixing device can be influential, leading us to melt PP at the process temperature prior to charging an EOC masterbatch containing cure formulation components. This technique ensures that curatives are incorporated uniformly and reproducibly, and it tends to concentrate cure chemistry within the EOC phase, thereby mitigating changes to the PP matrix.

Careful studies of the evolution of phase morphology during melt blending have established the importance of stresses imposed at polymer interface, which are, in turn, a function of shear rate, material viscosities, and interfacial tension. Our use of a Haake Polylab internal mixer operating at 60 RPM is consistent with most laboratory research[49], [50], and provides adequate dispersion without generating excessive melt temperatures due to viscous heating. Specific grades of PP and EOC were selected based on parent viscosities at 180°C and a shear rate of 50 s^{-1} (viscosity data provided in Appendix D), thereby ensuring that PP remained the continuous phase in all formulations.

Timescale of blend morphology development in melt blending processes has been studied extensively for unreactive[51]–[53], and reactive systems[8], [49], [54], [55]. For unreacted systems, final blend morphology can be achieved in less than one minute[8], [56], whereas reactive blend morphology develops with polyolefin modification[54]. Since materials are well-mixed within 1-2 min, DCP was selected to provide an adequate time period for mixing, and to avoid excessive thermal degradation. Given the half-life of DCP at 180°C is 0.86 min, peroxide-initiated reactions are essentially complete after 5 min. However, mechanically-induced generation of macroradicals can serve as a secondary, persistent source of radical activity, as can

conventional oxidation processes. Therefore, antioxidant was charged to the TPV after 5 min of reaction time, thereby stabilizing the product against further changes in polymer architecture.

Figure 5 provides plots illustrating the evolution of instrument torque and melt temperature for 70:30 wt:wt PP:EOC blends, with time zero established by the addition of the EOC masterbatch to pre-melted PP. Four formulations were examined. The unreactive system generated baseline data on blend morphology evolution for the starting materials, whereas the DCP-only formulation served as a control experiment illustrating the performance of a standard peroxide-mediated synthesis. TPVs prepared from DCP+AOTEMPO revealed the influence of the functional nitroxyl in isolation, while those produced by DCP+AOTEMPO+TMPTA demonstrated its influence in combination with a synergistic coagent.

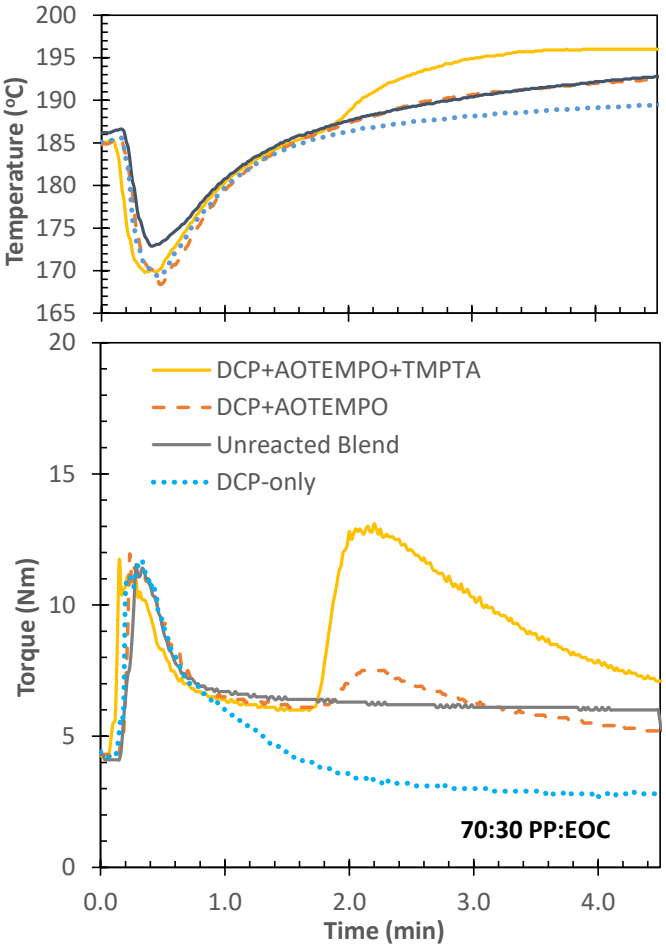

Figure 5 - Torque applied to 70:30 PP:EOC formulations during reactive compounding (60 RPM; T= 180°C).

The torque measurements plotted in Figure 5 are used widely as a proxy for steady-shear viscosity, and reflect changes in the rheological properties of each phase, as well as the blend morphology. Measurements for the unreactive blend reached a plateau within one minute of adding EOC, declining only slightly in response to changes in melt temperature. Note that an internal mixer does not provide isothermal conditions, since adding the EOC masterbatch absorbs heat in the early stages, and mechanical shear generates heat throughout the process. Data acquired for the DCP-only formulation demonstrated significant declines in torque over a

timescale consistent with peroxide decomposition over the observed melt temperature range. After 4.5 min of processing time, the resulting TPV generated torque values 50% lower than those of the unreactive blend. The cause of this decline, large scale degradation of the PP matrix, are discussed in the product characterization section that follows.

The DCP+AOTEMPO and DCP+AOTEMPO+TMPTA formulation data demonstrate the degree to which the dynamics and yields of a dynamic vulcanization can be controlled using a functional nitroxyl additive. In the early stages of these TPV syntheses, torque values were indistinguishable from those of the unreactive blend, as macroradical trapping by nitroxyl stabilized the melt viscosity of each phase while introducing pendant acrylate functionality. These chemical transformations take place concurrently with curative migration from the EOC masterbatch to the PP phase, and the development of a blend morphology. The latter is a distinguishing feature of our nitroxyl-mediated strategy, as it allows the starting materials to establish their inherent blend structure before the elastomer is rendered thermoset. As we demonstrated above, the induction time is a function of nitroxyl trapping ratio and the peroxide decomposition rate. Although the non-isothermal nature of a reactive compounding process makes it difficult to predict the induction time precisely, the transition from the induction phase to the oligomerization phase of the cure is easily identified by an abrupt rise in the applied torque.

This increase is the combined effect of changes in polymer rheology and blend morphology. Based on our study of individual blend components (Figure 4), polymer-bound acrylate oligomerization crosslinked the EOC phase extensively, while PP underwent simultaneous crosslinking and chain cleavage to varying extent depending on the availability of TMPTA

coagent. The torque profiles illustrated in Figure 5 show considerable reversion for both AOTEMPO formulations, presumably due to losses in PP matrix viscosity. More precise information regarding the rheological properties and morphology of these blends is provided below.

2.3.3 TPV Morphology Analysis

The morphology of our 70:30 samples were examined using scanning electron microscopy (SEM) to generate the images presented in Figure 6. All four materials were comprised of a continuous PP matrix, and a dispersed EOC phase, as expected given the predominant PP mass fraction. The dispersed phase morphology developed in the unreacted blend was quite uniform, with a mean droplet diameter of 1.7 μm and a PDI of 1.35. This degree of EOC droplet dispersion is consistent with expectations based on the relative viscosities of the blend components and their low interfacial free energy. The crosslinked EOC particles found in the TPV produce by peroxide alone were more irregularly shaped than the domains discovered in the unreactive blend. Nevertheless, this extent of EOC dispersion, with a mean particle diameter of 1.73 μm and a PDI of 1.22, approach those of TPVs reported for alternate chemistry[57].

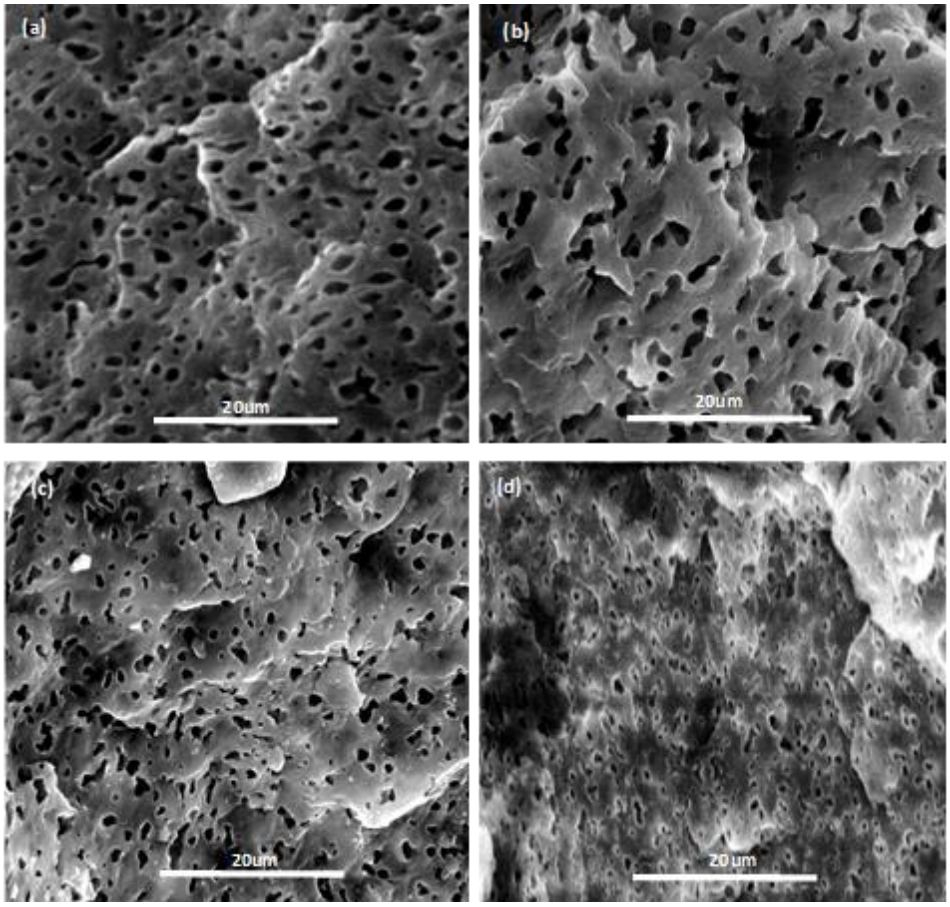

Figure 6 - SEM images of etched 70:30 blend surfaces: (a) unreacted, (b) peroxide, (c) peroxide + AOTEMPO, (d) peroxide + AOTEMPO + TMPTA.

The TPVs prepared from AOTEMPO formulations had unexpectedly good EOC phase dispersion. Our original concept for nitroxyl-mediated TPVs involved establishing the intrinsic blend morphology of the starting materials during an induction period, and "locking in" this morphology through a rapid oligomerization of acrylate functionality. However, the images presented in Figure 6 show that the nitroxyl-mediated TPVs possessed significantly better dispersion than the unreactive blend, with AOTEMPO alone producing EOC particles with diameters of 1.2 μm and a PDI of 1.18, and AOTEMPO+TMPTA generating 0.6 μm with a PDI of 1.28. Given that both nitroxyl formulations produced mixing torque values indistinguishable

from the unreactive blend up to the end of the induction period (Figure 5), it is clear that the blend morphology evolved during the oligomerization and uncontrolled modification phases of the cure process. We suggest that an increase in PP matrix viscosity, relative to peroxide only formulations, contributes to this morphology development, with the finer dispersion generated by AOTEMPO+TMPTA due, at least in part, to coagent-assisted PP crosslinking during the acrylate oligomerization phase.

The morphology trends observed in 70:30 blends were consistent for other PP:EOC ratios, with the nitroxyl-mediated formulations providing better EOC particle dispersions than unreactive blends and peroxide-only TPVs (Figure 7). Although particle diameters increased with the EOC weight fraction, the 50:50 materials retained a dispersed phase morphology, avoiding co-continuity. Images for 80:20, 60:40, and 50:50 blends can be found in Appendix A .

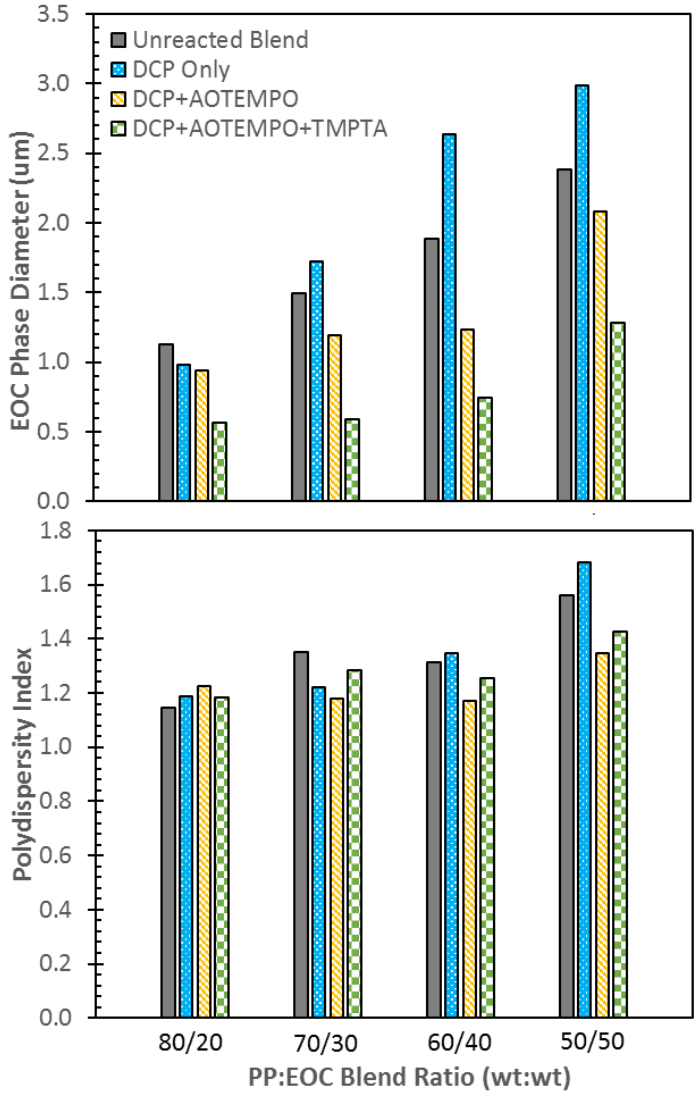

Figure 7 - Mean diameter of the EOC phase within various TPV products

2.3.4 TPV Rheology Analysis

Knowledge of melt-state rheological properties not only supports the development of polymer processing operations, it can provide insight into molecular weight distributions, chain architectures and blend morphologies. Given that PP was the continuous phase in all of our TPVs, an understanding of how chemical modification affects this polymer was needed before analyzing reactive PP+EOC blends. Figure 8a provides complex viscosity (η*), G', and phase angle

(degrees) measurements for unmodified PP and its derivatives. A detailed account of PP LCB effects on rheology can be found elsewhere[34], [35], [37]. Briefly, the starting material was a PP homopolymer whose high molecular weight was reflected by a relatively high complex viscosity and pronounced shear thinning character. Its linear structure limited its potential for chain entanglement, leading to relatively efficient stress relaxation at low frequency. This is evident in the approach of η^* toward a Newtonian plateau, and scaling of G' with ω^2, representing a terminal flow condition. As expected, peroxide-only degradation of this material lowered complex viscosity and storage modulus dramatically[58], while elevating low-frequency phase angle measurements toward $\delta=90^o$. This purely viscous response to an oscillatory deformation contrasts with that of a purely elastic material, for which the stress and strain are in-phase ($\delta=0^o$). Taken together, these rheology data are consistent with a low molecular weight, linear chain architecture[59], [60].

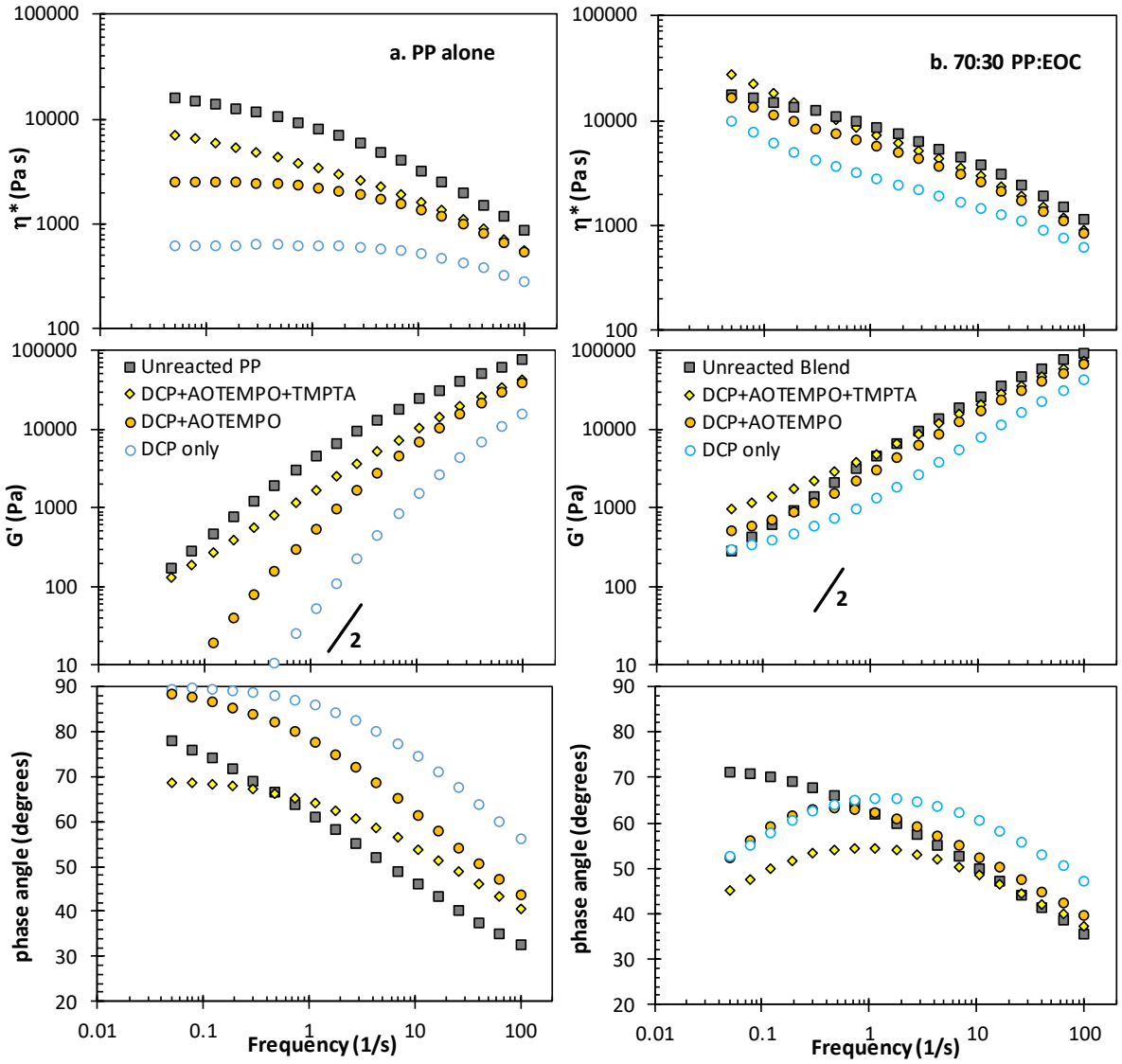

Figure 8 – η*, G', and phase angle versus frequency a. PP; b. 70:30 PP:EOC TPVs (170°C)

A stated objective of this work is to prepare peroxide-cured TPVs without compromising the molecular weight of the PP phase. The inclusion of AOTEMPO to a TPV formulation stabilizes the polymer's molecular weight during the induction period by macroradical trapping with nitroxyl functionality. During the subsequent oligomerization phase of the cure, activation of polymer-bound acrylate groups crosslinked the polymer concurrently with backbone

macroradical scission, the balance of which dictates the product molecular weight and branching distributions. Note that a perfect balance of chain growth and scission, such that the average molecular weight of the material is unchanged, will result in a different structure than the linear starting polymer. By design, an AOTEMPO formulation yields a LCB architecture, with obvious implications for melt rheological properties.

Applying DCP+AOTEMPO to PP alone gave a product whose complex viscosity and storage modulus were intermediate between the starting polymer and peroxide-degraded material (Figure 8a). Moreover, this PP derivative exhibited the Newtonian plateau and low-frequency phase angle of a substantially linear polymer. In contrast, the product of a DCP+AOTEMPO+TMPTA formulation showed unmistakable evidence of a long chain branched architecture, with low-frequency properties responding strongly to the stress relaxation restrictions arising from enhanced chain entanglement. Optimization of peroxide and nitroxyl loadings can be used to tailor these melt flow properties to achieve different outcomes, but as we noted above, adjustments to a TPV formulation must also consider potential changes to EOC crosslinking dynamics and yields.

Rheological data acquired for the 70:30 PP:EOC formulations are plotted in Figure 8b. Complex viscosity, storage modulus and phase angle measurements on the unreacted blend were similar to those made on the PP starting material, with only slight evidence of low-frequency elasticity that could be attributed to dispersed EOC droplets. In contrast, the peroxide-only TPV, while showing compelling indications of PP matrix degradation, demonstrated remarkable low-frequency elasticity. Given that radical-mediated PP degradation does not introduce significant amounts of

long chain branching, this diminished relaxation behaviour is attributed to the reinforcing effects of dispersed, cross-linked EOC particles. An early study of the steady shear rheology of conventional PP+EPDM TPVs characterized their behaviour as that of highly filled fluids, with the crosslinked phase serving as a particulate reinforcing agent[61]. This rheological model has been adopted by several subsequent studies of TPV systems[31], [32], [48]–[50], [62], and is consistent with the results of this work. Dispersed EOC particles eliminate the Newtonian plateau in the peroxide-only TPV, instead displaying an onset of yielding, and producing power-law behaviour over the entire studied frequency range.

These effects were most pronounced for the DCP+AOTEMPO+TMPTA formulation, which introduces long chain branching to the PP matrix while producing a fine dispersion of small EOC particles. However, it appears that the latter is more important to the melt-state rheology of nitroxyl-mediated TPV systems. The presence of EOC during the controlled curing process gives a product whose rheological properties approach those of unmodified PP, while producing the fine particle morphology required for a functional TPV material. The data plotted in Figure 9 expand the study to the other PP:EOC formulations. As expected, higher EOC contents result in greater reinforcing effects, with EOC loadings above 40 wt% producing rheological properties that exceeded those of the base PP resin.

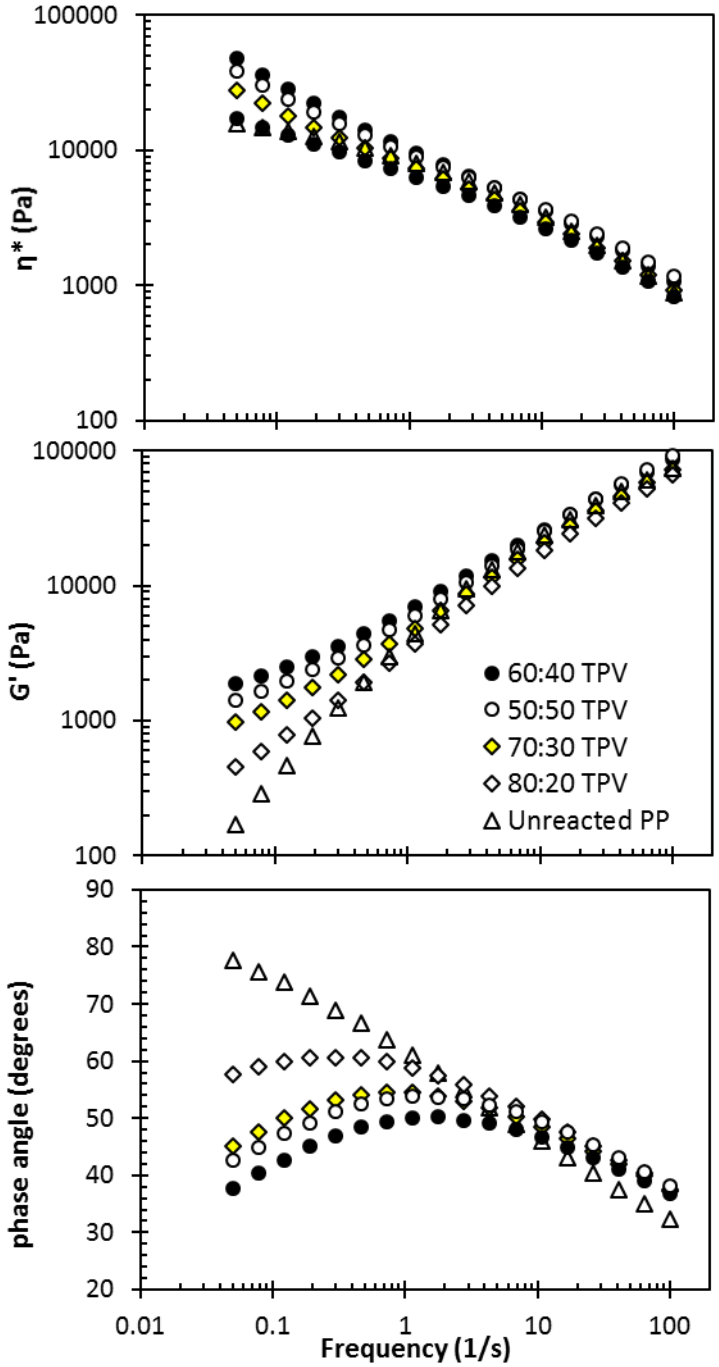

Figure 9 - Melt-state rheology data DCP+AOTEMPO+TMPTA applied to four PP:EOC blend ratios

2.4 Conclusions

Manufacturing of PP-rich TPVs using peroxides is hindered by the detrimental effects of radical degradation on PP matrix viscosity on TPV morphology. AOTEMPO-mediated formulations provide a means of controlling the dynamics of TPV processing and yields of polyolefin modification. The molecular weight of the continuous PP phase is maintained to a considerable extent by offsetting chain scission using macromonomer oligomerization, which is most effective when synergy between functionalized nitroxyls and coagents such as TMPTA is exploited. Although long chain branching is introduced by AOTEMPO formulations, melt rheological properties are dominated by dispersed phase particles, which act in a conventional filler reinforcement capacity.

Chapter 3

Rubber Toughening of Polypropylene using AOTEMPO

3.1 Introduction

PP is a semi-crystalline thermoplastic that is valued commercially for its low cost, chemical resistance, and favourable melt processing characteristics. Unfortunately, its relatively poor impact resistance makes PP ill-suited for a wide range of engineering applications, [31], [52], [63]–[65] but its brittleness can be mitigated by blending with elastomeric materials such as EPDM. The limited unsaturation content of this elastomer provides the thermooxidative stability needed to produce robust, long-lasting consumer goods [66]. This mature technology has been the subject of numerous studies of blend morphology, melt-state rheology, and solid-state mechanical properties [8], [66]–[68].

More recently, ultra-low density copolymers of ethylene and α-olefins such as octene (EOC) have attracted attention as PP blend components [1], [2], [49]. These elastomers typically provide narrow molecular weight distributions, uniform co-monomer distributions and short-chain branched architectures [2], [14]. Studies of thermoplastic olefin blends (TPOs) suggest that these mixtures can provide better toughness relative to conventional EPDM-based systems [69]. As noted in the introduction, dynamic vulcanization is a complex process wherein polyolefin modification occurs concurrently with blend morphology development. Elastomer droplet breakup and coalescence proceed as material properties evolve, until the dispersed phase is rendered thermoset. At this point, the material is a thermoplastic vulcanizate (TPV) and while coalescence is no longer operative, particle breakup can continue if mixing intensity is sufficient

[3]. The mechanical properties of PP:EOC TPVs are improved with smaller crosslinked particle sizes, and finer dispersions [3], [49], [70].

The previous chapter demonstrated the ability of acryloyloxy-2,2,6,6-tetramethylpiperidine-N-oxyl (AOTEMPO) to provide control over the dynamics and yields of a range of PP:EOC blends [21], [41], [42]. This chapter extends this research to the physical properties of TPVs containing relatively small amounts of EOC, with particular emphasis on impact resistance and mechanical stiffness.

3.2 Experimental

3.2.1 Materials

ESCORENE PP1042, an isotatic polypropylene homopolymer (MFR of 1.9 g/10min at 230°C), with a number average molecular weight of 96 kg/mol and a weight average molecular weight of 460 kg/mol [71], was obtained from ExxonMobil. A commercial grade poly(ethylene-co-octene) (Engage 8200), with 10 mol% octene[72], a density of 0.87 g/cm^3, and a MFR of 5.0 g/10min at 190 °C was supplied by DOW Chemical. 2,5-Bis(tert-butylperoxy)-2,5-dimethyl 3-hexyene (L130, 90%), acryloyl chloride (≥97%), triethylamine (≥99%), 4-hydroxy-2,2,6,6-tetramethylpiperidin-1-oxyl (TEMPOH, 97%), and pentaerythritol tetrakis(3,5-di-tert-butyl-4-hydroxyhydrocinnamate) (Irganox1010, 98%) were used as received from Sigma-Aldrich.

3.2.2 AOTEMPO Synthesis

A solution of triethylamine (706 mg, 0.97 mL, 6.98 mmol) in benzene (12.0 mL) was added dropwise to a solution of TEMPOH (0.688 g, 4.40 mmol) in benzene (10.0 mL). Acryloyl chloride (0.374 g, 340 μL, 4.16 mmol) in benzene (7.0 mL) was added dropwise at room

temperature, under N_2 with stir. The reaction was stirred at room temperature for 20 h before the second portion of acryloyl chloride (0.188 g, 170 µL, 2.08 mmol) in benzene (3.5 mL) was added dropwise. The reaction was stirred at room temperature for an additional hour. Resulting solution was filtered before removing solvent under vacuum, yielding orange crystals that were recrystallized from cyclohexane. Yield: 76%; mp 100-102 °C; lit. 102-104 °C[45].

3.2.3 TPV Synthesis

Polymer blends were produced by mixing PP and EOC (PP:EOC compositions by weight include: 80:20, 90:10, 95:05. 100:0) with an acetone solution containing L130 (0.5 wt%, 17.45 µmol/g) and when applicable AOTEMPO (29.3 µmol/g). Samples were allowed to dry prior to adding the material to a Haake Polylab R600 internal batch mixer. Samples were allowed to mix and vulcanize for 14 min at 60RPM before adding Irganox 1010 (0.5 wt%, 4.25 µmol/g) to stabilize for one minute. Unreactive blends were then quenched using ice-water to preserve the morphology and avoid annealing.

3.2.4 Rheological Analysis

Base polymers were cured using a controlled-strain rheometer (Advanced Polymer Analyzer 2000, Alpha Technologies) equipped with biconical plates operating at 180°C, 1Hz, 3° arc. Samples were prepared by coating, hand mixing, and drying 5 g of ground polymer with an acetone solution containing L130 (17.45 µmol/g) and AOTEMPO (loadings ranged from 0 – 35.2 µmol/g).

A controlled strain rheometer (Anton Parr MCR301) with 25 mm diameter parallel plates, with a 1 mm gap, was used in oscillatory mode, at 170 °C, and 3% strain to measure TPV rheological

characteristics. Stress sweeps were performed to ensure all data acquired was within the linear viscoelastic region.

3.2.5 Morphological Analysis

Samples were immersed in liquid nitrogen for 5 min before fracturing. Surfaces of interest were etched for 2.5 hr using heptane at 80 °C. Unreacted blends were immediately dried under vacuum at 60 °C for 10 hr, while TPVs were sonicated using a Misonix XL2000 microson ultrasonic probe for three 1 min intervals at a power output of 22 watts before drying. All etched samples were gold-coated and imaged using a Hitachi S-2300 scanning electron microscope. Images were analyzed using ImageJ, imaging analysis software, to estimate the diameter of the dispersed elastomer phase.

3.2.6 Mechanical Properties Measurements

Notched Izod impact tests were carried out according to ASTM D256 using a Instron BLI impact tester at room temperature. Specimens (dimensions 62.5 x 12.5 x 3.1 mm^3) were prepared by compression molding at 180°C. Flexural tests were performed according to ASTM D790 at a speed of 1.3 mm/min. Rectangular bars (dimensions 125 x 13.1 x 3.05 mm^3) were prepared by compression molding at 180°C. Tensile properties were measured using an Instron 3369 universal tester at crosshead speed of 25 mm/min. Dumbbell-shaped specimens with an average thickness of 1.8 mm, were cut with a type-V die according to ASTM D638. A minimum of three samples were tested for each composition and formulation with average values being reported with standard deviations.

3.3 Results and Discussion

3.3.1 Individual Polyolefin Modification

Although TPV manufacturing is a dynamic process where polyolefin modification occurs simultaneously with melt mixing, knowledge of how each blend component responds to curative formulations is needed to develop appropriate peroxide cure formulations. This study began with rheology studies of EOC and PP individually, in which G' at constant temperature, frequency, and amplitude (180°C, 1Hz, and 3° arc, respectively) was monitored as a function of time. The data plotted in Figure 10a show that an EOC formulation comprised of L-130 alone crosslinked the polymer with characteristic first-order kinetics to generate a net gain of $\Delta G'$=150 kPa. In contrast, a L130-only formulation of PP formulation resulted in substantial polymer degradation, with a net loss of $\Delta G'$=-15 kPa over the same period (Figure 10b). Clearly, the challenge in producing a TPV from PP+EOC is to generate the requisite elastomer crosslink density while minimizing losses in thermoplastic matrix viscosity.

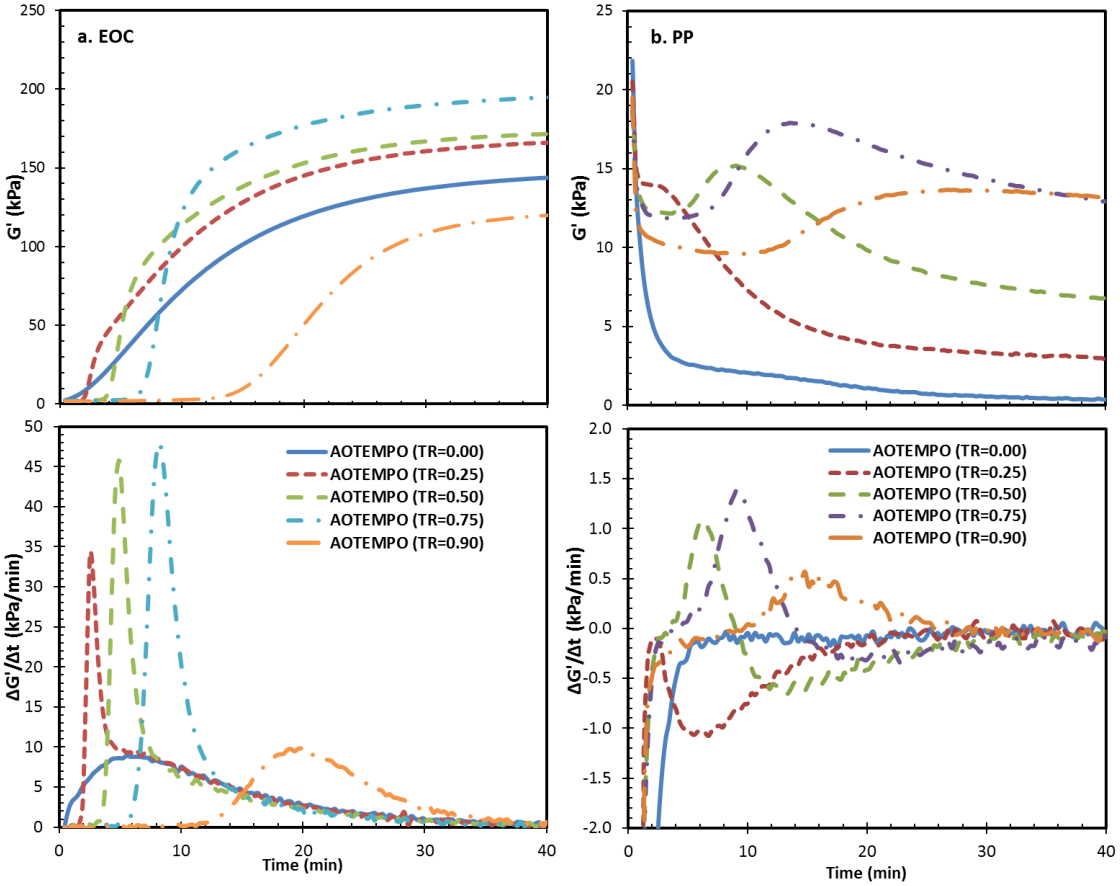

Figure 10 – Effect of TR on evolution of G' and dG'/dt for peroxide-intiated polyolefin modification (a) EOC, (b) PP; [L130] = 17.45 µmol/g, 180 °C, 1 Hz, and 3 °arc.

The principles of AOTEMPO-mediated PP and EOC modifications have been described in Chapter 2, and are well demonstrated by the data plotted in Figure 10. Irrespective of the polymer structure, increasing the AOTEMPO trapping ratio (TR = [AOTEMPO]/(4*[L130]) lengthened the observed induction period. In the case of EOC, higher TR values raised the crosslink density of EOC significantly, in keeping with observations made by Hyslop and Parent[42] on analogous LLDPE formulations, until such point (TR ≥ 0.9), that insufficient peroxide initiator was available during phase 2 to convert polymer-bound acrylate functionality.

As expected, applying AOTEMPO to the PP system mitigated the extent of polymer degradation, with a TR = 0.75 providing an ultimate ΔG'=-0.6 kPa.

A summary of induction time and ΔG' data derived from EOC and PP rheology measurements is plotted in Figure 11. The induction times correspond closely to values calculated from equation 1, which is derived assuming isothermal reaction conditions and fast, irreversible trapping of carbon-centered radicals by the nitroxyl.

$$t_{ind} = -\frac{1}{k_d}\ln(1 - \frac{[nitroxyl]}{4[L130\}}) \qquad \text{Eq 1.}$$

This relationship makes it a simple straightforward matter to select the trapping ratio that is needed to meet an induction time target. However, given the sensitivity of the ultimate EOC crosslink density and PP melt viscosity on the AOTEMPO loading, the TR used for a TPV preparation must consider reaction outcomes. Based on the ΔG' data plotted in Figure 11, TR=0.75 was selected for continued study. This nitroxyl concentration provided a high extent of EOC crosslinking while minimizing the extent of PP degradation. Furthermore, it should provide an induction time of 7.2 min to allow blend morphology to develop under parent material properties. Note that reaction conditions provided by the rheometer are isothermal, but nearly free of applied strain. DV, on the other hand, raises the melt temperature continuously by viscous heating while providing intense dispersive and distributive mixing. Therefore, formulations optimized for individual blend components in a parallel plate rheometer may not be optimal for a DV process. It is likely that the formulation can be refined by trial and error experimentation.

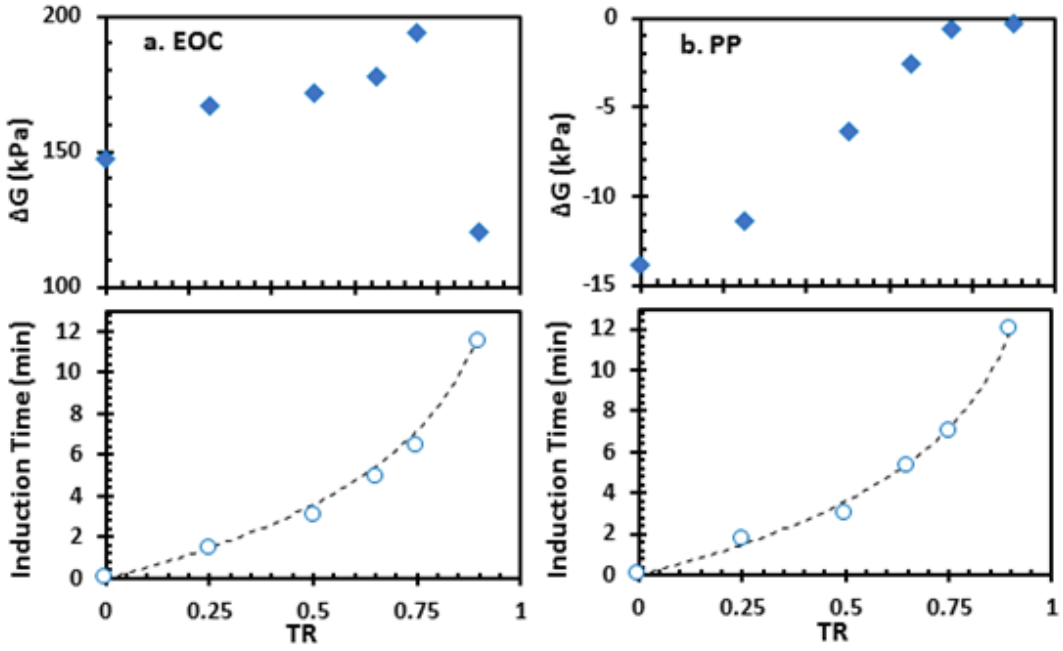

Figure 11 - Storage modulus changes and induction times recorded as a function of AOTEMPO trapping ratio (a. EOC; b. PP; T=180ºC; dashed line represents equation 1).

3.3.2 TPV Processing

The evolution of blend morphology in an unreactive system depends on several variables including: the amounts and viscosities of the parent materials, the interfacial tension between components, and the shear and extensional strains imposed by the mixing process [3], [5], [6]. Mixing was accomplished with a Haake Polylab internal mixer operating at 180°C and 60 RPM, which is consistent with other laboratory research in TPV manufacturing [49], [73]. The starting materials were selected to have similar melt viscosities at this processing temperature (viscosity data available in Appendix D) to ensure that dispersive mixing occurred efficiently during the induction period provided by AOTEMPO. TPV formulations were prepared by solution-coating 40 g batches of ground polymer with an acetone solution of peroxide + additive, and allowing the masterbatch to dry before charging to the preheated instrument.

Time measurements of the torque applied by the internal mixer to the TPV formulation are used widely to monitor changes in rheological properties as DV proceeds. Figure 12 shows torque and melt temperature data acquired for three cure formulations applied to a 80:20 PP:EOC blend ratio. The unreactive (curative-free) blend reached a torque plateau after two minutes of melt mixing, declining only slightly as the melt temperature increased. The peroxide-only formulation resulted in a net loss of 6.2 Nm in torque after six minutes of compounding, likely due to degradation of the continuous PP matrix. In contrast, the AOTEMPO-mediated vulcanization provided a 6 minute induction period, after the torque spiked 5 Nm, presumably as acrylate oligomerized in both phases, before giving way to uncontrolled radical degradation of the PP continuous phase.

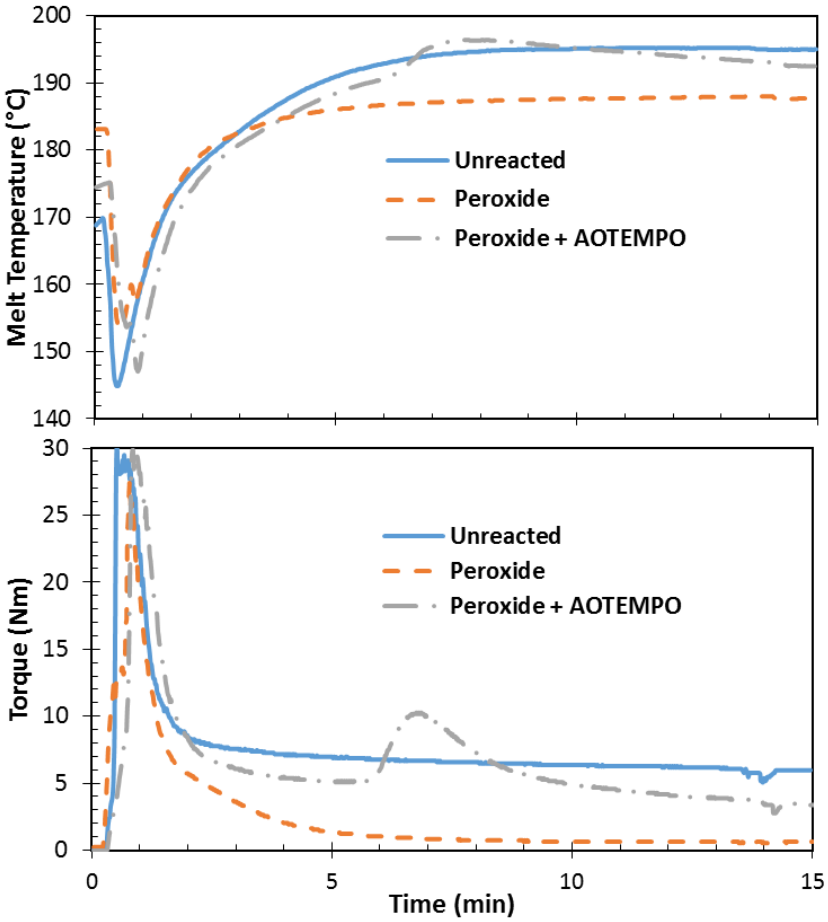

Figure 12 - Evolution of torque and melt temperature for 80:20 PP:EOC formulations during reactive compounding (T-180 °C, 60 RPM)

TPVs designed for structural applications that require impact resistance usually contain less than 10 wt% elastomer, which if sufficiently dispersed, provides the necessary balance between material stiffness and toughness. Therefore, two additional blend ratios were prepared, providing at total of three formulations for further analysis: 95:05, 90:10, and 80:20. Each of these blend ratios was formulated free of curatives (unreacted blend), with peroxide alone, and with peroxide + AOTEMPO. The morphology and melt rheological properties of the resulting materials were characterized before examining solid-state impact, flexural and tensile properties.

3.3.3 Morphological Analysis

SEM analysis of samples that had been fractured, etched, and sonicated provided information on the morphology of unreactive PP:EOC blends and TPVs. The images provided in Figure 13 confirm that all materials were comprised of a continuous matrix of PP combined with a dispersed EOC phase. Unreactive blends with low EOC content contained a uniform distribution of sub-micron droplet sizes, with mean diameters of 157 ± 9.6 nm for the 95:05 material, and 164 ± 11.1 nm for the 90:10 mixture (Figure 13a). This fine dispersion is consistent with conventional knowledge of polymer blends, given the viscosity ratio between the PP and EOC starting materials, and their low interfacial free energy. However, raising the EOC composition to 20 wt% resulted in a much coarser morphology, as the 80:20 blend produced a mean droplet diameter of 450 ± 54 nm. The droplets become larger with increased elastomer content, resulting from heightened coalescence during melt-processing, and is an intrinsic property of this particular compounding mixture/process. It should be recognized, however, that the morphology of these unreacted blends can shift if subjected to further melt processing operations, as annealing studies have demonstrated coalescence of droplets in the absence of shear [74].

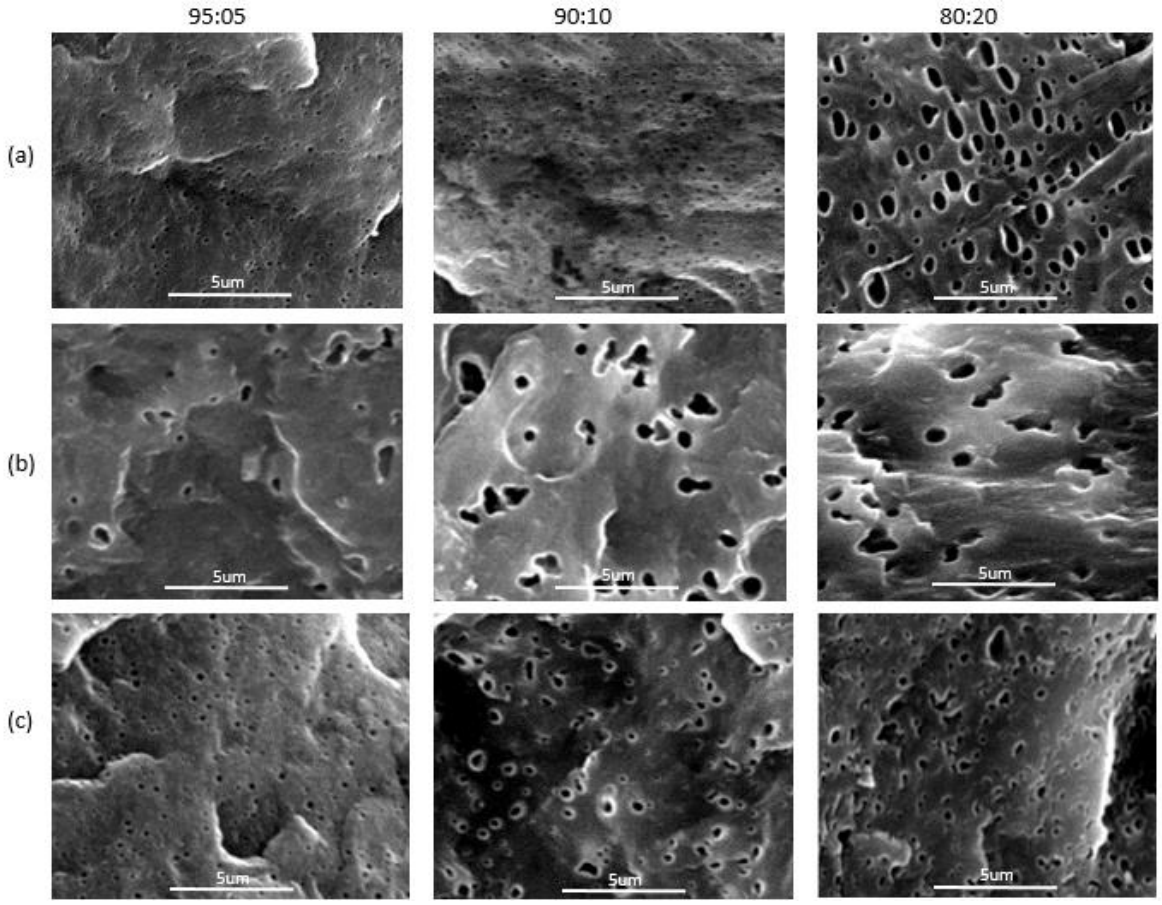

Figure 13 – SEM images of etched samples: (a) unreacted blends, (b) peroxide, (c) peroxide + AOTEMPO

Although peroxide-only formulations produce crosslinked particles that are not susceptible to coalescence, they produced a much coarser morphology than the unreactive blends. The images provided in Figure 13b reveal TPVs comprised of relatively large, irregularly-shaped particles with broad size distributions. A plot of dispersed-phase dimensions produced by the various formulations highlights the mediocre performance of peroxide alone (Figure 14). Degradation of the PP matrix reduces stress transfer to the PP-EOC interface, while EOC crosslinking increases the resistance of the dispersed phase to breakup. This shift in viscosity ratio leads to the larger

particles sizes observed in this work,[75], [76] and raises concerns for the impact resistance of these TPVs [6], [51].

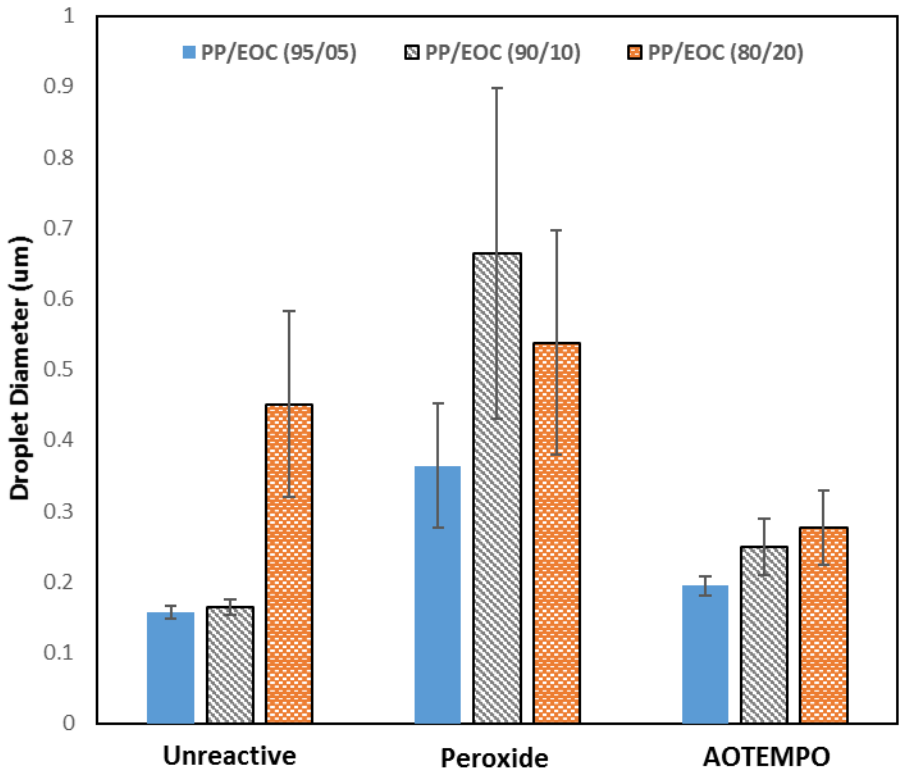

Figure 14 – Average EOC phase diameters

AOTEMPO formulations produced acceptable morphologies for all of the PP:EOC compositions. SEM images (Figure 13c) revealed narrow particle size distributions with averages ranging from 190 ± 15 nm for the 95:05 blend ratio to 275 ± 50 nm for the 80:20 blend ratio (Figure 14). The consistent performance of the AOTEMPO system can be attributed to the induction period that allows a fine blend morphology to develop, and the retention of PP melt viscosity throughout the DV process.

3.3.4 Melt State Rheology

Insight into the molecular structure of homopolymers and their blends can be gained from studies of melt-state rheological properties. Figure 15 provides plots of η*, G', and phase angle against oscillation frequency for PP as well as the 90:10 PP:EOC system. Data for the 95:05 and 80:20 compositions are available as Appendix B.

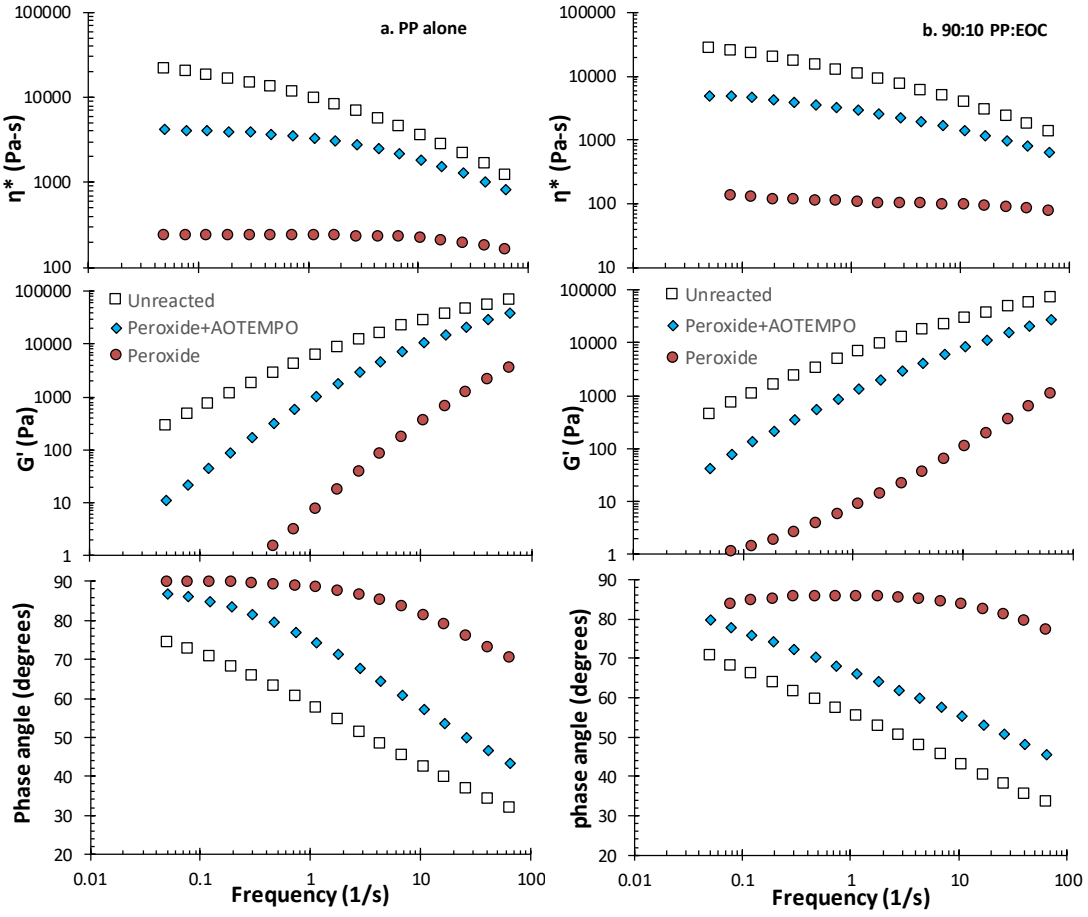

Figure 15 – η*, G' and phase angle versus frequency (a. PP; b. PP:EOC = 90:10; T=170ºC)

This data is consistent with our previous study of the PP+EOC system, as PP degradation by peroxide alone resulted in severely diminished chain entanglement, as reflected by losses of η*

and G'. The AOTEMPO formulations mitigated these changes to a considerable extent by building molecular weight during the oligomerization phase of the cure. However, this molecular weight growth produces a branched architecture whose rheological properties can differ considerably from those of the linear starting material [35], [37]. The data plotted in Figure 15 show little evidence of long chain branching in the PP derivatives, and only weak evidence of EOC particle reinforcing effects in the TPV.

Higher EOC loadings, including the 80:20 composition examined in this study, show rheological behaviour that is consistent with filler-reinforced composites [31], [49], [61], [62]. This includes heightened elasticity at low oscillation frequencies, and power-law viscosity relationships in the place of Newtonian flow behaviour. However, the absence of these effects in the 90:10 TPV suggests that impact-modified materials can be made to have similar rheological behaviour to that of the unfilled PP starting material, as long as the required impact resistance can be gained using small amounts of crosslinked EOC.

3.3.5 Physical Property Assessments

This study concludes with an investigation of the solid-state physical properties of the three blend formulations. Figure 16 summarizes the results of (a) impact, (b) flexural, and (c,d) tensile testing. Additional physical property data are available as Appendix C. Since the main motivation for producing a PP-based TPV is to improve impact resistance, the notched Izod impact measurement of the PP starting material (50 J/m, Figure 16a) is the benchmark to which all formulations must be compared. This value can be obtained from "as received" resin without blending or chemical modification. As expected, preparing unreacted PP blends with increasing amounts of EOC enhances impact resistance, with just 10% EOC providing a 3.5-fold

improvement over PP alone. Although unreactive blending is effective, the morphology of these materials can be unstable during further melt processing, leading to droplet coalescence and compromised physical properties[74].

Crosslinking of EOC droplets to produce thermoset particles produces a stable morphology, but without a guarantee of improved impact resistance. For example, TPVs produced with a peroxide-only formulation could not exceed the benchmark until the EOC content was raised to 20 wt%. This performance limitation is a product of PP matrix degradation, coupled with a coarse blend morphology. The AOTEMPO formulation was much more effective, with the 90:10 PP:EOC system providing a 2.2-fold improvement in impact resistance over the PP parent material. Just as was observed for the unreactive blend, raising the EOC content to 20 wt% produced a “hinge-break” test result. This is unfortunate, since the AOTEMPO formulation produced a finer morphology for this composition than the unreactive system, which is expected to produce a better impact result [51].

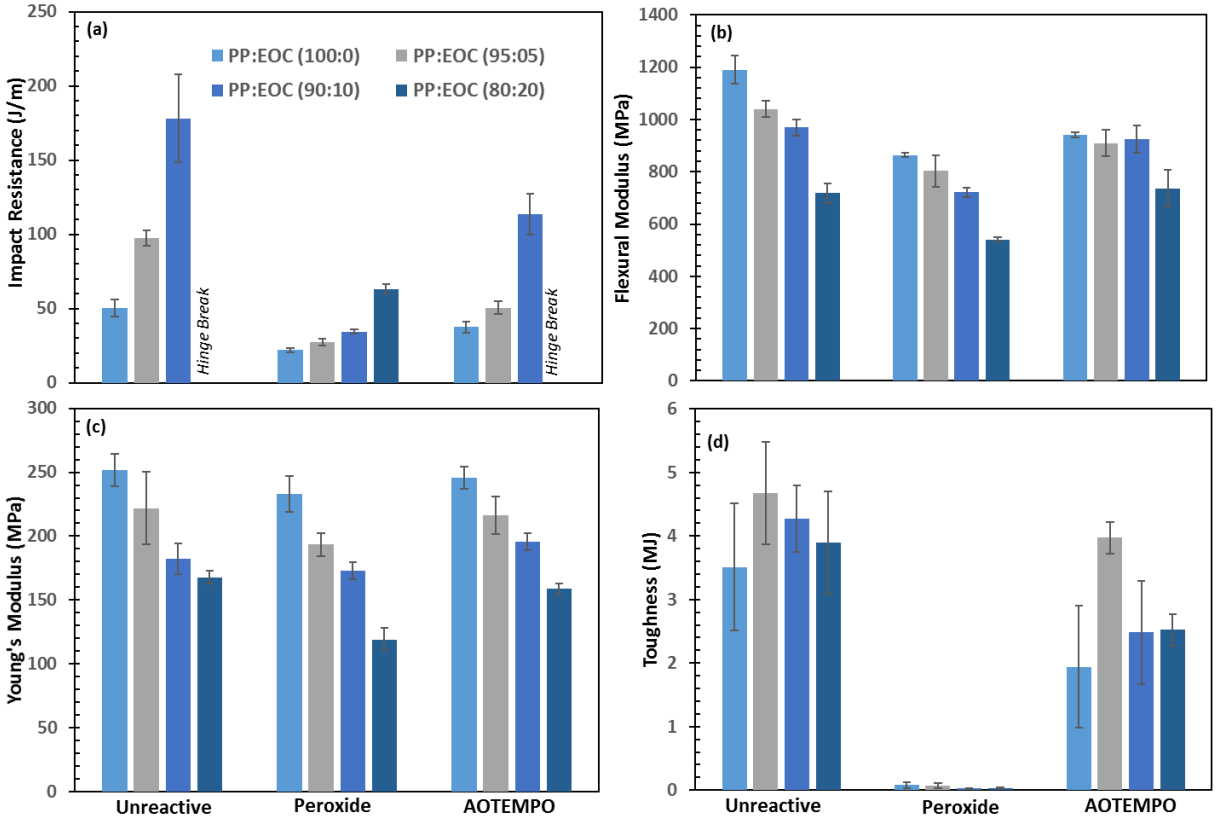

Figure 16 – Comparison of chemical formulations on physical property performance of unreacted blends and TPVs: (a) impact resistance, (b) flexural modulus, (c) Young's modulus, (d) toughness.

It is generally recognized that the dispersion of an elastomer in PP improves impact resistance at the expense of mechanical strength/rigidity [77]. This is demonstrated by the flexural and Young's modulus data plotted in Figure 16(b,c), which show depreciated stiffness with increasing EOC content. Figure 16(d) compares the toughness, the area under a stress-extension curve, for all formulations across all polymer compositions. Knowledge of the relationship between the molecular weight of a polymer and its tensile stress-strain response is well developed, with high MW materials enduring greater elongation to break and providing better ultimate tensile strength

[39], [40]. It is not surprising, therefore, that the toughness of peroxide-only formulations was compromised by a low elongation at break arising from severe PP matrix degradation. TPVs prepared with AOTEMPO provided much better toughness/ductility than can be realized using peroxide alone, as the retention of PP molecular weight, and the introduction of long chain branching enhanced chain entanglements.

3.4 Conclusions

Peroxide vulcanization of PP-rich TPVs is hindered by PP's susceptibility to radical degradation. AOTEMPO-mediated formulations provide PP melt viscosity retention by introducing a competition between β-scission and in situ macromonomer oligomerization. Resulting formulations provide superior particle sizes and dispersion in comparison to peroxide-only formulations. Improved impact performance and retention of tensile properties observed for AOTEMPO formulations attributed to reduced PP degradation. Preservation of molecular weight allowed finer dispersions to be achieved (impact improvements), and provided more chain entanglements within the matrix (retention of tensile properties).

Chapter 4

Conclusions and Future Work

4.1 AOTEMPO-Mediated Synthesis of TPVs

Dynamic vulcanization of PP-rich TPVs is hindered by PP's susceptibility to radical degradation, resulting in substantial losses in melt viscosity, producing coarser morphologies. Our work focused on using AOTEMPO to control the dynamics of TPV compounding, and stabilize PP melt viscosity by introducing a competition between macromonomer oligomerization and chain scission. Further improvements were realized by synergizing AOTEMPO with TMPTA, a trifunctional coagent. Copolymerization of polymer bound functionality with TMPTA's acrylate functionality provide a more extensive C-C network within both EOC and PP phases. TPVs manufactured with AOTEMPO provided improved particle sizes and dispersions when compared to peroxide-only formulations. Optimal results were obtained with the combination of both AOTEMPO and TMPTA.

4.2 Rubber Toughening of Polypropylene using AOTEMPO

PP-based TPVs containing low elastomer content (0-20wt%) were produced using AOTEMPO-mediated peroxide vulcanization. Resulting materials had smaller average particle sizes, and finer dispersions when compared to peroxide-only formulations, owing to the retention of melt viscosity. Finer morphologies resulted in improved physical property performance, with AOTEMPO-mediated TPVs possessing superior impact properties than peroxide-only. Furthermore, tensile properties were partially retained for AOTEMPO blends, likely resulting from the modifications to the PP's chain architecture. Linear chains are expected to transform by simultaneous chain scission and in situ macromonomer oligomerization. This variation in

architecture will provide more chain entanglements than the peroxide only formulations, explaining the improved tensile properties observed

4.3 Future Work

4.3.1 Nitroxyl-mediated Strategies to Introduce LCB

Commercial PP's linear structure can be transformed into a LCB architecture, which is more desirable when melt strength and elongational viscosity are important material properties[78]. A simple single-step method of achieving this modification is to use peroxide initiated grafting of a multifunctional coagent such as TMPTA. This process involves simultaneous PP chain scission and coagent-induced crosslinking, with the balance dictating the extent of branching formed. A variety of coagents have been proven capable of introducing LCB but many are limited by their inability to provide uniform branching[35], [36]. For example, PP modification with DCP and triallyl trimesate (TAM) resulted in a bimodal distribution of chains, with the bulk material degrading, and a small population of hyperbranched chains forming[34].

We have demonstrated AOTEMPO capability of grafting to the PP backbone, during the induction phase through macroradical combination, and its ability to synergize with multifunctional coagents such as TMPTA. Additionally, our preliminary rheology data of peroxide modified PP (Chapter 2, Figure 8a), showed pronounce LCB effects with the combination of AOTEMPO and TMPTA. However, a more in-depth analysis is needed to further characterize the LCB extent. High temperature triple detection GPC is a common method used to evaluate the molecular weight distribution of a polymer, and has been used previously in LCB studies[34]. It is recommended to use GPC in tandem with rheological characterization

(frequency sweeps, extensional viscosity measurements) to evaluate functionalized nitroxyls capability in providing a more uniform branch distribution than coagent-only formulations.

4.3.2 High Rubber Content TPVs

This thesis focused on the effect AOTEMPO of TPVs with elastomer content ranging from 0-50wt%. In these cases, the blend morphology of the parent materials starts out as either co-continuous or with PP as the continuous matrix. However high elastomer content (60-80wt%) TPVs can be produced, but have a more complex morphology evolution, with the elastomer phase initially being the continuous phase. If high crosslink densities are achieved, the elastomer phase will end up as dispersed crosslinked particles through a phase inversion process, while lightly crosslinked systems will achieve “soft TPVs” with the elastomer phase remaining the continuous matrix. An immediate extension of this work would be to investigate the performance of AOTEMPO on these blends, and determine how the morphology evolution would be effected by the nitroxyl chemistry.

References

[1] M. Kontopoulou, W. Wang, T. G. Gopakumar, and C. Cheung, "Effect of composition and comonomer type on the rheology, morphology and properties of ethylene-α-olefin copolymer/polypropylene blends," *Polymer (Guildf).*, vol. 44, no. 24, pp. 7495–7504, 2003.

[2] T. McNally, P. McShane, G. M. Nally, W. R. Murphy, M. Cook, and A. Miller, "Rheology, phase morphology, mechanical, impact and thermal properties of polypropylene/metallocene catalysed ethylene 1-octene copolymer blends," *Polymer (Guildf).*, vol. 43, no. 13, pp. 3785–3793, 2002.

[3] K. Naskar, "Dynamically vulcanized PP/EPDM thermoplastic elastomers. Exploring novel routes for crosslinking with peroxides," University of Twente, The Netherlands, 2004.

[4] S. Abdou-Sabet, R. C. Puydak, and C. P. Rader, "Dynamically Vulcanized Thermoplastic Elastomers," *Rubber Chem. Technol.*, vol. 69, no. 3, pp. 476–494, Jul. 1996.

[5] G. M. Jordhamo, J. A. Manson, and L. H. Sperling, "Phase continuity and inversion in polymer blends and simultaneous interpenetrating networks," *Polym. Eng. Sci.*, vol. 24, no. 8, p. 1327, 1986.

[6] S. Wu, "Formation of dispersed phase in incompatible polymer blends: Interfacial and rheological effects," *Polym. Eng. Sci.*, vol. 27, no. 5, pp. 335–343, Mar. 1987.

[7] G. N. Avgeropoulos, F. C. Weissert, P. H. Biddison, and G. G. A. Böhm, "Heterogeneous blends of polymers. Rheology and morphology," *Rubber Chem. Technol.*, vol. 49, no. 1, pp. 93–104, 1976.

[8] C. F. Antunes, A. V. MacHado, and M. Van Duin, "Morphology development and phase inversion during dynamic vulcanisation of EPDM/PP blends," *Eur. Polym. J.*, vol. 47, no.

7, pp. 1447–1459, 2011.

[9] M. Van Duin, “Chemistry of EPDM crosslinking,” *kautschuk gummi kunststoffe*, vol. 55, no. 4, pp. 150–156, 2002.

[10] H. G. Fritz, U. Bolz, and Q. Cai, “Innovative TPV two-phase polymers: Formulation, morphology formation, property profiles and processing characteristics,” *Polym. Eng. Sci.*, vol. 39, no. 6, pp. 1087–1099, 1999.

[11] J. F. Schombourg, P. Kraxner, W. Furrer, and A. Adberrazig, “Silane vulcanized thermoplastic elastomers.” Patents US 6448343 B1, 2002.

[12] M. van Duin and A. Souphanthong, “The chemistry of phenol-formaldehyde resin vulcanization of EPDM: Part I. Evidence for methylene crosslinks,” *Rubber Chem. Technol.*, vol. 68, no. 5, pp. 717–727, 1995.

[13] M. van Duin, “The chemistry of phenol-formaldehyde resin crosslinking of EPDM as studied with low-molecular-weight models: Part II. Formation of inert species, crosslink precursors and crosslinks,” *Rubber Chem. Technol.*, vol. 73, no. 4, pp. 706–719, Sep. 2000.

[14] K. L. Walton, “Metallocene catalyzed ethylene/alpha olefin copolymers used in thermoplastic elastomers,” *Rubber Chem. Technol.*, vol. 77, no. 3, pp. 552–568, 2004.

[15] D. V Avila, U. Ingold, and J. Lusztyk, “Solvent effects on the competitive β-scission and atom abstraction reactions of the cumyloxyl radical. Resolution of a long-standing problem,” *J. Am. Chem. Soc.*, vol. 115, pp. 466–470, 1993.

[16] B. M. Molloy, “Functionalized-nitroxyls for use in peroxide-initiated modifications of polymers,” Queen’s University, 2014.

[17] K. U. Ingold, “Rate constants for free radicals in solution,” *New York Intersci.*, p. 92,

1973.

[18] H. Hamilton, E.J.J., Fisher, “Electron spin resonance measurement of radical termination rates,” *J. Phys. Chem.*, vol. 77, pp. 722–724, 1973.

[19] F. Romania, R. Corrieri, V. Bragab, and F. Ciardelli, “Monitoring the chemical crosslinking of propylene polymers through rheology,” *Polymer (Guildf).*, vol. 43, no. 4, pp. 1115–1131, 2001.

[20] S. Mani, P. Cassagnau, M. Bousmina, and P. Chaumont, “Crosslinking control of PDMS rubber at high temperatures using TEMPO nitroxide,” *Macromolecules*, vol. 42, no. 21, pp. 8460–8467, 2009.

[21] B. M. Molloy, D. K. Hyslop, and J. S. Parent, “Comparative analysis of delayed-onset peroxide crosslinking formulations,” *Polym. Eng. Sci.*, vol. 54, no. 11, pp. 2645–2653, 2014.

[22] P. Hudec and L. Obdržálek, “The change of molecular weights at peroxide initiated degradation of polypropylene,” *Die Angew. Makromol. Chemie*, vol. 89, no. 1, pp. 41–45, Aug. 1980.

[23] C. Tzoganakis, Y. Tang, J. Vlachopoulos, and A. E. Hamielec, “Controlled degradation of polypropylene: A comprehensive experimental and theoretical investigation,” *Polym. Plast. Technol. Eng.*, vol. 28, no. 3, pp. 319–350, 1989.

[24] G. E. Garrett, E. Mueller, D. A Pratt, and J. S. Parent, “Reactivity of polyolefins toward cumyloxy radical: yields and regioselectivity of hydrogen atom transfer,” *Macromolecules*, vol. 47, pp. 544–551, 2014.

[25] I. Chodák and M. Lazár, “Effect of the type of radical initiator on crosslinking of polypropylene,” *Die Angew. Makromol. Chemie*, vol. 106, no. 1, pp. 153–160, Jul. 1982.

[26] I. Chodák and E. Zimányová, “The effect of temperature on peroxide initiated crosslinking of polypropylene,” *Eur. Polym. J.*, vol. 20, no. 1, pp. 81–84, Jan. 1984.

[27] G. Alvarez, “Novel co-agents for improved properties in peroxide cure of saturated elastomers,” University of Twente, The Netherlands, 2007.

[28] J. A. Cornell, A. J. Winters, and L. Halterman, “Mechanism of rubber coagent peroxide cure system,” *Rubber Chem. Technol.*, vol. 43, no. 3, pp. 613–623, May 1970.

[29] G. Hulse, R. Kerstring, and D. Warfel, “Chemistry of dicumyl peroxide induced crosslinking of linear polyethylene,” *J. Polym. Sci. Polym. Chem. Ed.*, vol. 19, pp. 655–667, 1981.

[30] R. R. Babu, N. K. Singha, and K. Naskar, “Phase morphology and melt rheological behavior of uncrosslinked and dynamically crosslinked polyolefin blends: Role of macromolecular structure,” *Polym. Bull.*, vol. 66, no. 1, pp. 95–118, 2011.

[31] R. R. Babu, N. K. Singha, and K. Naskar, “Interrelationships of morphology, thermal and mechanical properties in uncrosslinked and dynamically crosslinked PP/EOC and PP/EPDM blends,” *Express Polym. Lett.*, vol. 4, no. 4, pp. 197–209, 2010.

[32] R. Rajesh Babu, N. K. Singha, and K. Naskar, “Influence of 1,2-polybutadiene as coagent in peroxide cured polypropylene/ethylene octene copolymer thermoplastic vulcanizates,” *Mater. Des.*, vol. 31, no. 7, pp. 3374–3382, 2010.

[33] H. H. Winter, “Can the gel point of a crosslinking polymer be detected by the G’-G" crossover?,” *Polym. Eng. Sci.*, vol. 27, no. 22, pp. 1698–1702, 1987.

[34] J. S. Parent, S. S. Sengupta, M. Kaufman, and B. I. Chaudhary, “Coagent-induced transformations of polypropylene microstructure: Evolution of bimodal architectures and cross-linked nano-particles,” *Polymer (Guildf).*, vol. 49, no. 18, pp. 3884–3891, 2008.

[35] K. El Mabrouk, J. S. Parent, B. I. Chaudhary, and R. Cong, “Chemical modification of PP architecture: Strategies for introducing long-chain branching,” *Polymer (Guildf).*, vol. 50, no. 23, pp. 5390–5397, 2009.

[36] Y. Zhang, P. Tiwary, J. S. Parent, M. Kontopoulou, and C. B. Park, “Crystallization and foaming of coagent-modified polypropylene: Nucleation effects of cross-linked nanoparticles,” *Polymer (Guildf).*, vol. 54, no. 18, pp. 4814–4819, 2013.

[37] J. S. Parent, A. Bodsworth, S. S. Sengupta, M. Kontopoulou, B. I. Chaudhary, D. Poche, and S. Cousteaux, “Structure-rheology relationships of long-chain branched polypropylene: Comparative analysis of acrylic and allylic coagent chemistry,” *Polymer (Guildf).*, vol. 50, no. 1, pp. 85–94, 2009.

[38] G. G. A. Böhm and M. DOLE, “The Radiation Chemistry of Elastomers,” Academic Press, 1972, pp. 195–260.

[39] S. Wu, “Chain structure, phase morphology, and toughness relationships in polymers and blends,” *Polym. Eng. Sci.*, vol. 30, no. 13, pp. 753–761, 1990.

[40] C. Tzoganakis, J. Vlachopoulos, A. E. Hamielec, and D. M. Shinozaki, “Effect of molecular weight distribution on the rheological and mechanical properties of polypropylene,” *Polym. Eng. Sci.*, vol. 29, no. 6, pp. 390–396, 1989.

[41] D. K. Hyslop and J. S. Parent, “Functional nitroxyls for use in delayed-onset polyolefin crosslinking,” *Macromolecules*, vol. 45, pp. 8147–8154, 2012.

[42] D. K. Hyslop and J. S. Parent, “Dynamics and yields of AOTEMPO-mediated polyolefin cross-linking,” *Polymer (Guildf).*, vol. 54, no. 1, pp. 84–89, 2013.

[43] K. Premphet and W. Paecharoenchai, “Polypropylene/metallocene ethylene-octene copolymer blends with a bimodal particle size distribution: Mechanical properties and

their controlling factors," *J. Appl. Polym. Sci.*, vol. 85, no. 11, pp. 2412–2418, 2002.

[44] P. Tiwary, H. Gui, P. L. Ferreira, and M. Kontopoulou, "Coagent modified polypropylene prepared by reactive extrusion: A new look into the structure-property relations of injection molded parts," *Int. Polym. Process.*, vol. 31, no. 4, pp. 433–441, 2016.

[45] J. Zakrzewski, "Reactions of nitroxides XIII: Synthesis of the Morita-Baylis-Hillman adducts bearing a nitroxyl moiety using 4-acryloyloxy-2,2,6,6- tetramethylpiperidine-1-oxyl as a starting compound, and DABCO and quinuclidine as catalysts," *Beilstein J. Org. Chem.*, vol. 8, pp. 1515–1522, 2012.

[46] G. Pan, B. Zu, X. Guo, Y. Zhang, C. Li, and H. Zhang, "Preparation of molecularly imprinted polymer microspheres via reversible addition-fragmentation chain transfer precipitation polymerization," *Polymer (Guildf).*, vol. 50, no. 13, pp. 2819–2825, 2009.

[47] K. Naskar and J. W. M. Noordermeer, "Dynamically vulcanized PP/EPDM blends: Effects of different types of peroxides on the properties," *Rubber Chem. Technol.*, vol. 76, no. 4, p. 1001=1018, 2003.

[48] R. R. Babu, N. K. Singha, and K. Naskar, "Effects of mixing sequence on peroxide cured polypropylene (PP)/ethylene octene copolymer (EOC) thermoplastic vulcanizates (TPVs). Part. II. Viscoelastic characteristics," *J. Polym. Res.*, vol. 18, no. 1, pp. 31–39, 2011.

[49] Z. Li and M. Kontopoulou, "Evolution of rheological properties and morphology development during crosslinking of polyolefin elastomers and their TPV blends with polypropylene," *Polym. Eng. Sci.*, vol. 49, no. 1, pp. 34–43, 2009.

[50] H. Ezzati, Peyman, Ghasemi, Ismaeil, Karrabi, Mohammad, Azizi, "Rheological behaviour of PP/EPDM blend: The effect of compatibilization," *Iran. Polym. J.*, vol. 17, no. 9, pp. 669–679, 2009.

[51] S. Wu, “Phase structure and adhesion in polymer blends: A criterion for rubber toughening,” *Polymer (Guildf).*, vol. 26, no. 12, pp. 1855–1863, 1985.

[52] J. Karger - Kocsis, A. Kallo, A. Szafner, G. Bodor, and Z. Senyei, “Morphological study on the effect of elastomeric impact modifiers in polypropylene systems,” *Polym. (United Kingdom)*, vol. 20, no. 1, pp. 37–43, 1979.

[53] G. M. Brown and J. H. Butler, “New method for the characterization of domain morphology of polymer blends using ruthenium tetroxide staining and low voltage scanning electron microscopy (LVSEM),” *Polymer (Guildf).*, vol. 38, no. 15, pp. 3937–3945, 1997.

[54] H. Wu, M. Tian, L. Zhang, H. Tian, Y. Wu, N. Ning, and T. W. Chan, “New understanding of morphology evolution of thermoplastic vulcanizate (TPV) during dynamic vulcanization,” *ACS Sustain. Chem. Eng.*, vol. 3, no. 1, pp. 26–32, 2015.

[55] H. Wu, M. Tian, L. Zhang, H. Tian, Y. Wu, and N. Ning, “New understanding of microstructure formation of the rubber phase in thermoplastic vulcanizates (TPV),” *Soft Matter*, vol. 10, no. 11, pp. 1816–1822, 2014.

[56] F. Goharpey, A. A. Katbab, and H. Nazockdast, “Formation of rubber particle agglomerates during morphology development in dynamically crosslinked EPDM/PP thermoplastic elastomers. Part 1: effects of processing and polymer structural parameters,” *Rubber Chem. Technol.*, vol. 76, no. 1, pp. 239–252, 2003.

[57] M. D. Ellul, A. H. Tsou, and W. Hu, “Crosslink densities and phase morphologies in thermoplastic vulcanizates,” *Polymer (Guildf).*, vol. 45, no. 10, pp. 3351–3358, 2004.

[58] F. Berzin, B. Vergnes, and L. Delamare, “Rheological behavior of controlled-rheology polypropylenes obtained by peroxide-promoted degradation during extrusion: Comparison

between homopolymer and copolymer," *J. Appl. Polym. Sci.*, vol. 80, no. 8, pp. 1243–1252, 2001.

[59] S. Trinkle, P. Walter, and C. Friedrich, "Van Gurp-Palmen Plot II - classification of long chain branched polymers by their topology," *Rheol. Acta*, vol. 41, no. 1–2, pp. 103–113, 2002.

[60] G. Barakos, E. Mitsoulis, C. Tzoganakis, and T. Kajiwara, "Rheological characterization of controlled-rheology polypropylenes using integral constitutive equations," *J. Appl. Polym. Sci.*, vol. 59, no. 3, pp. 543–556, 1996.

[61] L. A. Goettlier, J. R. Richwine, and F. J. Wille, "The rheology and processing of olefin-based thermoplastic vulcanizates," *Rubber Chem. Technol.*, vol. 55, no. 5, pp. 1448–1463, Nov. 1982.

[62] B. Kuriakose and S. K. De, "Studies on the melt flow behavior of thermoplastic elastomers from polypropylene-natural rubber blends," *Polym. Eng. Sci.*, vol. 25, no. 10, pp. 630–634, 1985.

[63] K. C. Dao, "Rubber phase dispersion in polypropylene," *Polymer (Guildf).*, vol. 25, no. 10, pp. 1527–1533, 1984.

[64] J. Karger-Kocsis, A. Kallo, and V. N. Kuleznev, "Phase structure of impact-modified polypropylene blends," *Polym. (United Kingdom)*, vol. 25, no. 2, pp. 279–286, 1984.

[65] A. van der Wal, J. J. Mulder, J. Oderkerk, and R. J. Gaymans, "Polypropylene–rubber blends: 1. The effect of the matrix properties on the impact behaviour," *Polym. (United Kingdom)*, vol. 39, no. 26, pp. 6781–6787, 1998.

[66] M. Van Duin, "Recent developments for EPDM-based thermoplastic vulcanisates," *Macromol. Symp.*, vol. 233, pp. 11–16, 2006.

[67] A. Thitithammawong, C. Nakason, K. Sahakaro, and J. Noordermeer, “Effect of different types of peroxides on rheological, mechanical, and morphological properties of thermoplastic vulcanizates based on natural rubber/polypropylene blends,” *Polym. Test.*, vol. 26, no. 4, pp. 537–546, 2007.

[68] H. Goharpey, F. Katbab, A.A. Nazockdast, “Mechanism of morphology development in dynamically cured EPDM/PP TPEs. I. Effects of state of cure,” *J. Appl. Polym. Sci.*, vol. 81, no. 10, pp. 2531–2544, 2001.

[69] A. L. N. Da Silva, M. C. G. Rocha, F. M. B. Coutinho, R. Bretas, and C. Scuracchio, “Rheological, mechanical, thermal, and morphological properties of polypropylene/ethylene-octene copolymer blends,” *J. Appl. Polym. Sci.*, vol. 75, no. 5, pp. 692–704, 2000.

[70] D. Bacci, R. Marchini, and M. T. Scrivani, “Constitutive equation of peroxide crosslinking of thermoplastic polyolefin rubbers,” *Polym. Eng. Sci.*, vol. 45, no. 3, pp. 333–342, 2005.

[71] Y. Zhang, P. Tiwary, H. Gui, M. Kontopoulou, and J. S. Parent, “Crystallization of coagent-modified polypropylene: Effect of polymer architecture and cross-linked nanoparticles,” *Ind. Eng. Chem. Res.*, vol. 53, no. 41, pp. 15923–15931, 2014.

[72] K. Premphet and W. Paecharoenchai, “Polypropylene/metallocene ethylene-octene copolymer blends with a bimodal particle size distribution: Mechanical properties and their controlling factors,” *J. Appl. Polym. Sci.*, vol. 85, pp. 2412–2418, 2002.

[73] F. Goharpey, H. Nazockdast, and A. A. Katbab, “Relationship between the rheology and morphology of dynamically vulcanized thermoplastic elastomers based on EPDM/PP,” *Polym. Eng. Sci.*, vol. 45, no. 1, pp. 84–94, 2005.

[74] S. H. Lee, M. Bailly, and M. Kontopoulou, “Morphology and properties of

poly(propylene)/ethylene-octene copolymer blends containing nanosilica," *Macromol. Mater. Eng.*, vol. 297, no. 1, pp. 95–103, 2012.

[75] J. Karger-Kocsis and V. N. Kuleznev, "Dynamic mechanical and impact properties of polypropylene/EPDM blends," *Polymer (Guildf).*, vol. 23, no. 5, pp. 699–705, 1982.

[76] B. P. Panda, S. Mohanty, and S. K. Nayak, "Mechanism of toughening in rubber toughened polyolefin — A review," *LPTE*, vol. 54, no. 5, pp. 462–473, 2015.

[77] F. C. Stehling, T. Huff, and C. S. Speed, "Structure and properties of rubber-modified polypropylene impact blends," vol. 26, pp. 2693–2711, 1981.

[78] R. Hingmann and B. L. Marczinke, "Shear and elongational flow properties of polypropylene melts," *J. Rheol. (N. Y. N. Y).*, vol. 38, no. 3, pp. 573–587, May 1994.

Appendix A

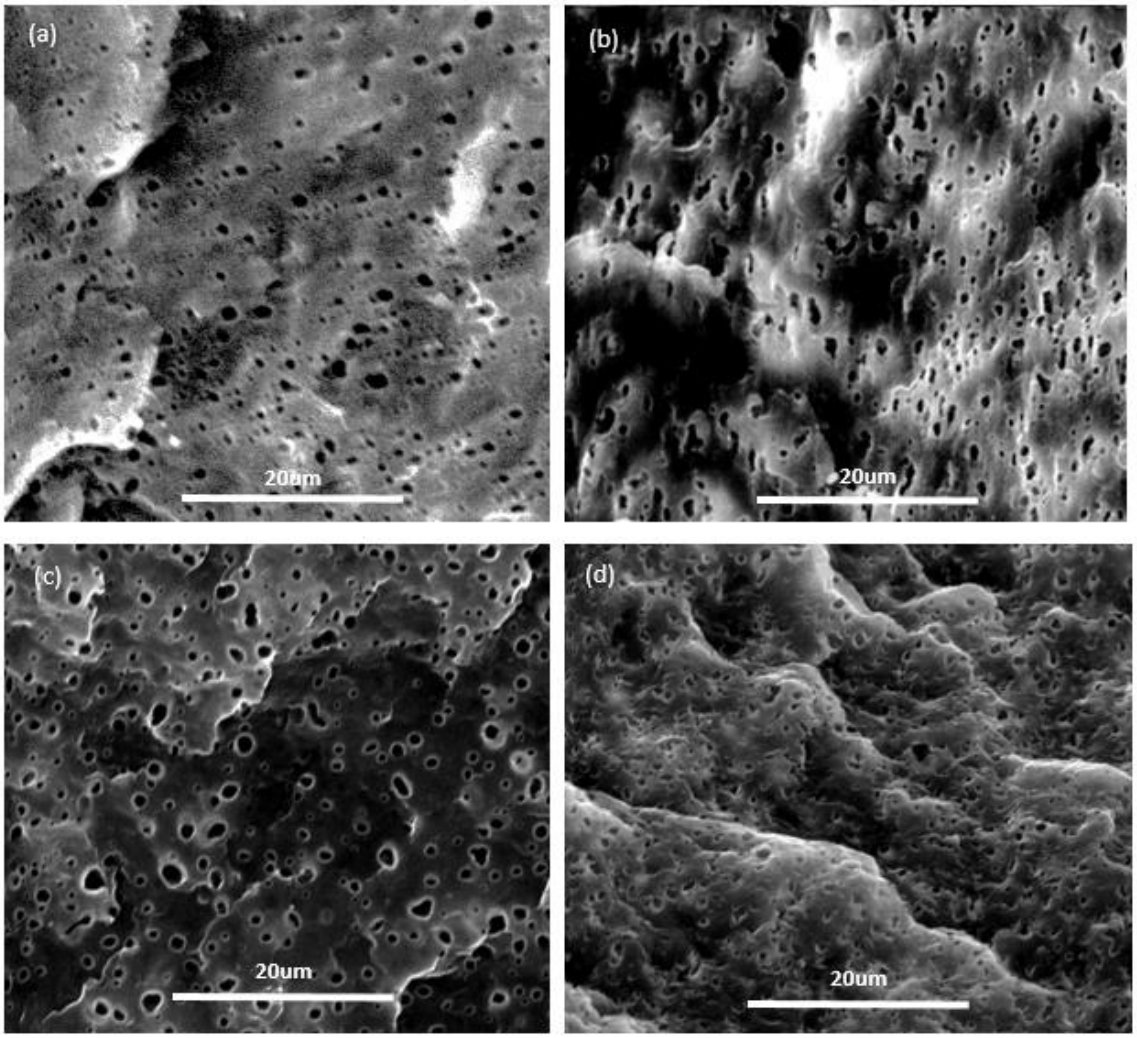

Figure 17 – SEM images of etched 80:20 blend surfaces: (a) unreacted, (b) peroxide, (c) peroxide + AOTEMPO, (d) peroxide + AOTEMPO + TMPTA.

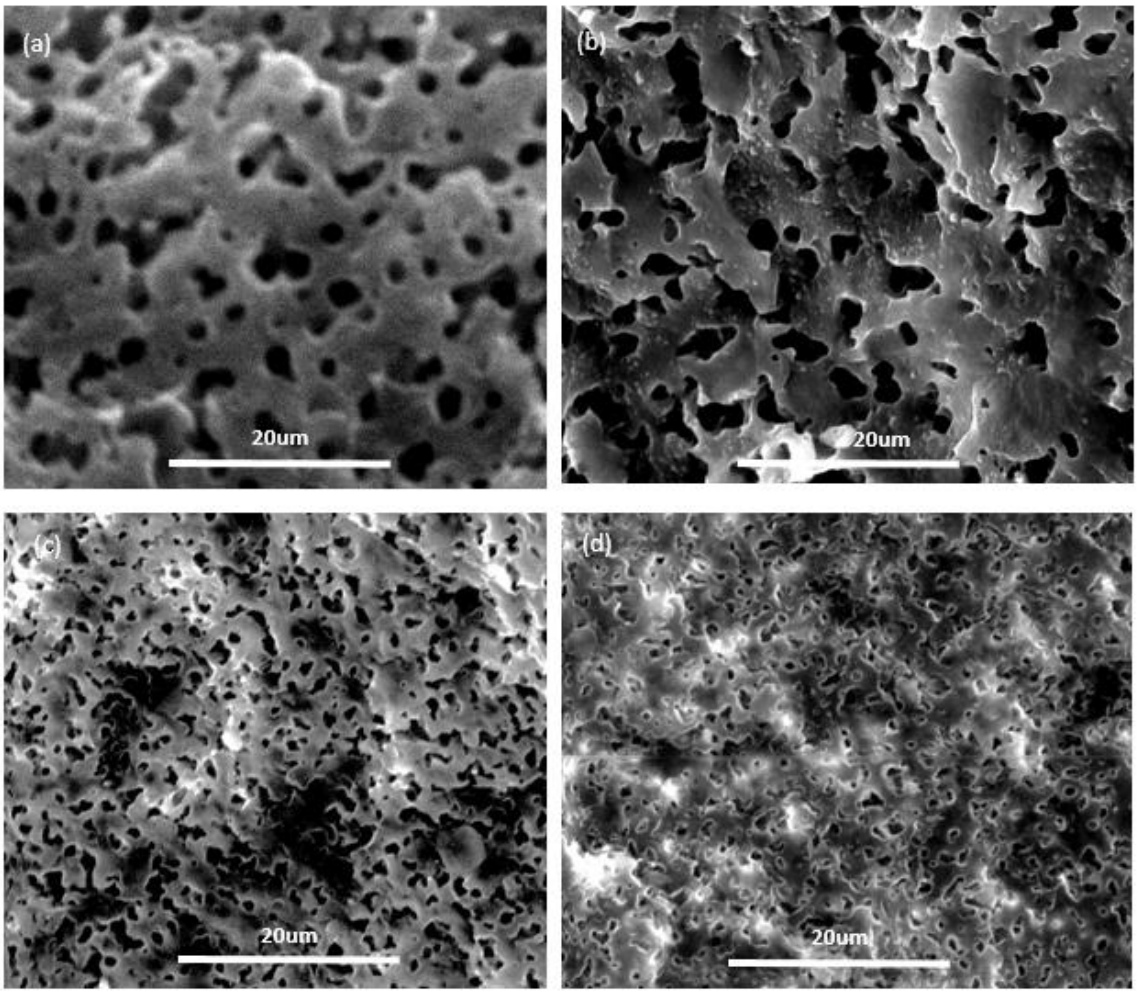

Figure 18 - SEM images of etched 60:40 blend surfaces: (a) unreacted, (b) peroxide, (c) peroxide + AOTEMPO, (d) peroxide + AOTEMPO + TMPTA.

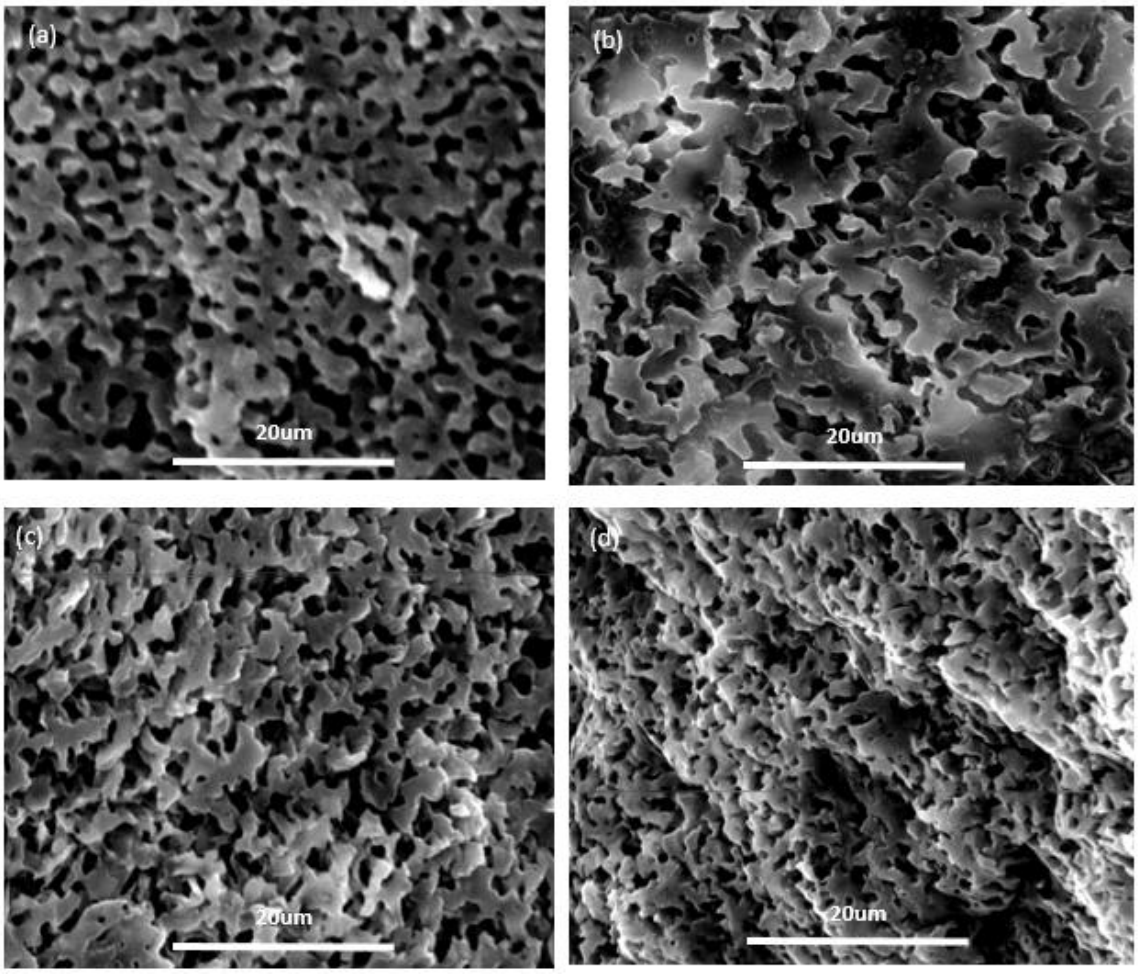

Figure 19 - SEM images of etched 50:50 blend surfaces: (a) unreacted, (b) peroxide, (c) peroxide + AOTEMPO, (d) peroxide + AOTEMPO + TMPTA.

Appendix B

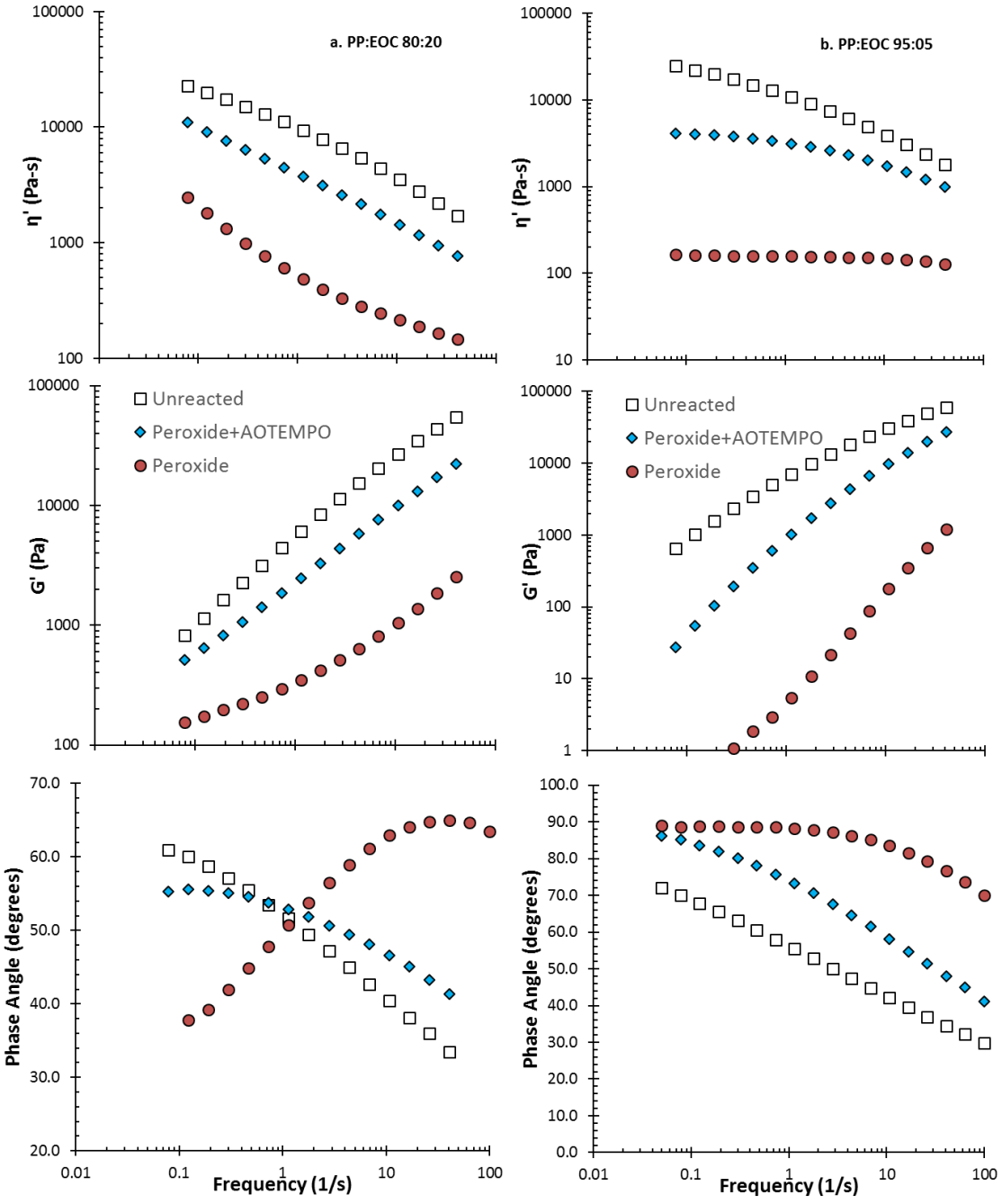

Figure 20 - η*, G' and phase angle versus frequency (a. 80:20; b. 95:05; T=170ºC)

Appendix C

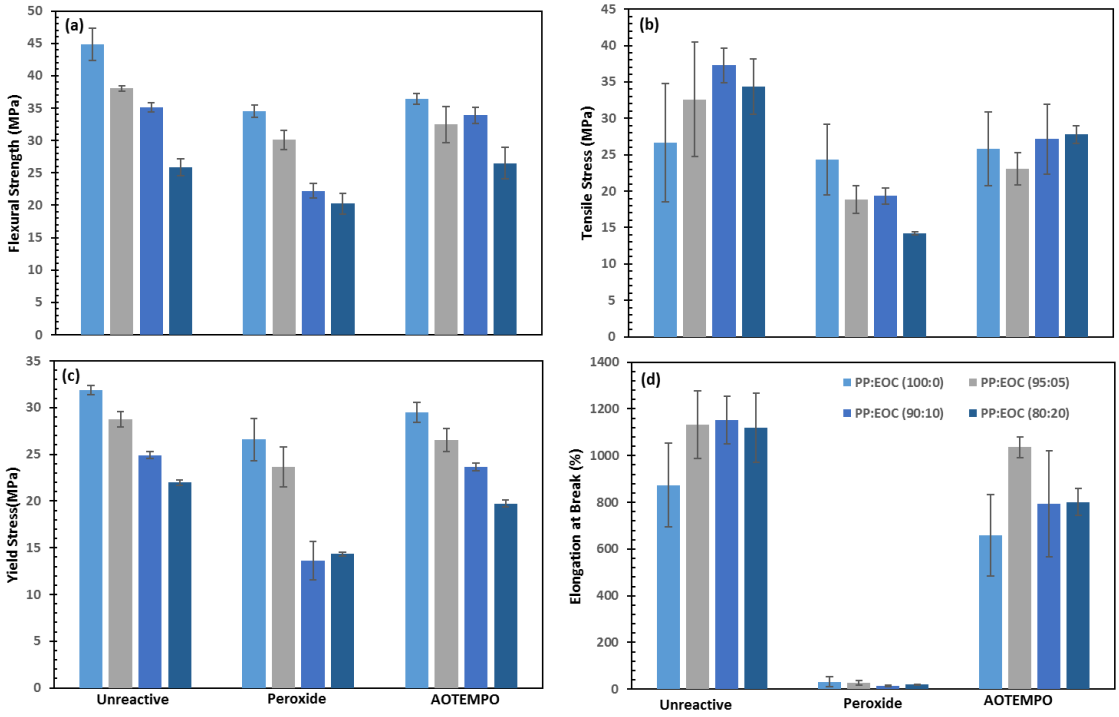

Figure 21 – Supplemental Physical Property Data

Appendix D

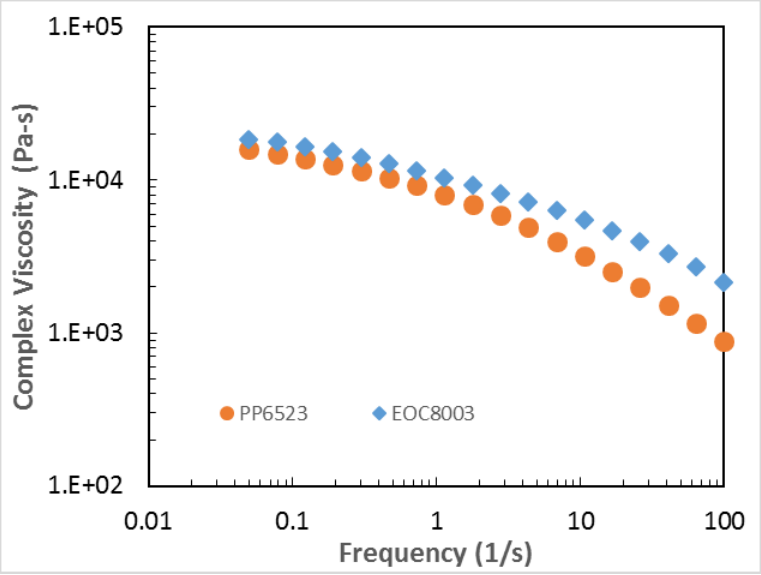

Figure 22 – Frequency sweep of parent materials

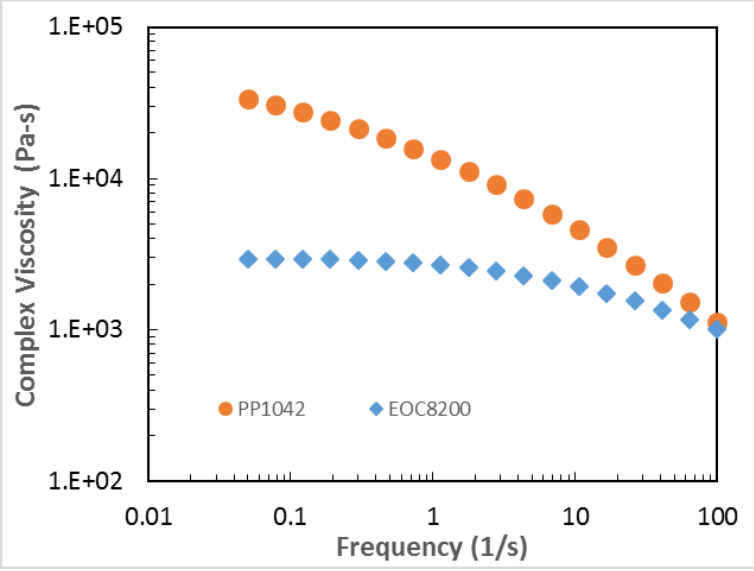

Figure 23 - Frequency sweep of parent materials